Part One

Fundamentals of Fluidization

Chapter 1

A Description of Fluidized Bed Behaviour

An introduction to fluidization

Consider a bed of particulate solids or powder, say of a size similar to table salt. When a fluid, either a gas or a liquid, is passed upwards through the bed, the bed particles remain stationary or packed at low fluid velocities. This is a packed or fixed bed. If now the velocity of the fluid is increased, the particles will begin to separate and move away from one another; the bed is said to expand. On increasing the velocity further, a point will be reached at which the drag force exerted by the fluid on a particle is balanced by the net weight of the particle. The particles are now suspended in the upward-moving stream of fluid. This is the point of minimum fluidization, or incipient fluidization, at and beyond which the bed is said to be fluidized.

The superficial fluid velocity in the bed at the point of incipient fluidization is called the minimum fluidizing velocity u_{mf} and is of crucial importance in characterising the behaviour of a fluidized bed. Superficial velocity is defined as the volumetric flow rate of fluid divided by the cross-sectional area of the bed. In other words, superficial velocity is equal to the mean fluid velocity assuming that the particles are not present; the actual interstitial fluid velocity will, of course, be somewhat higher. At velocities in excess of that required for minimum fluidization one of two phenomena will occur. First, the bed may continue to expand and the particles space themselves uniformly. This is known as particulate, or homogeneous, fluidization (Figure 1.1) and in general occurs when the fluidizing medium is a liquid. Alternatively, the excess fluid, beyond that required to achieve fluidization, may pass through the bed in the form of bubbles. The particles are agitated and mixed, violently so at higher velocities, and the bubbles rise through the bed to break at the surface. This is called aggregative, bubbling or heterogeneous fluidization and usually occurs where the fluidizing medium is a gas. It is this type of behaviour which gives rise to the analogy of a boiling liquid (Figure 1.2).

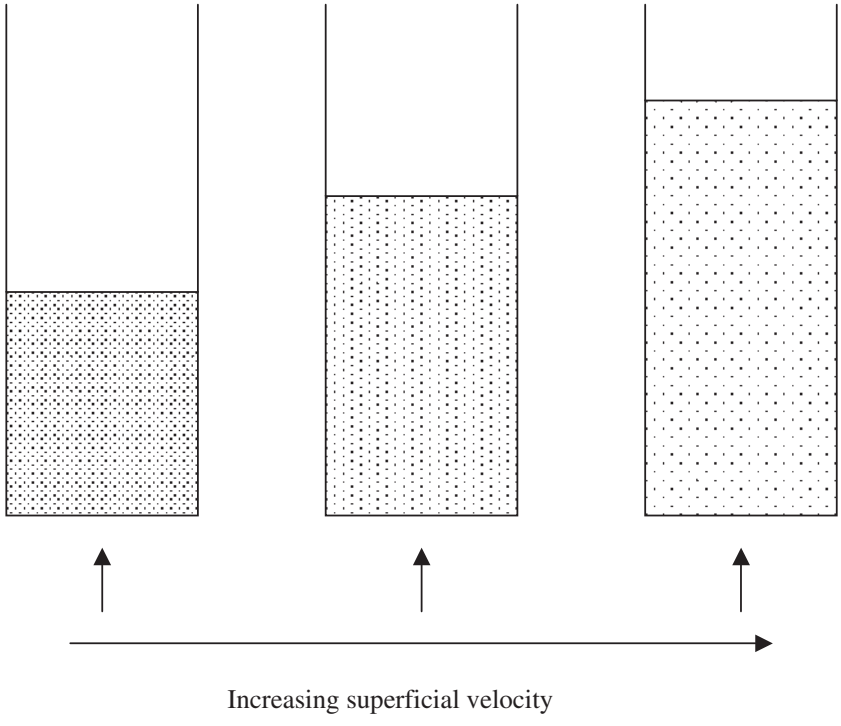

Figure 1.1 Particulate fluidization.

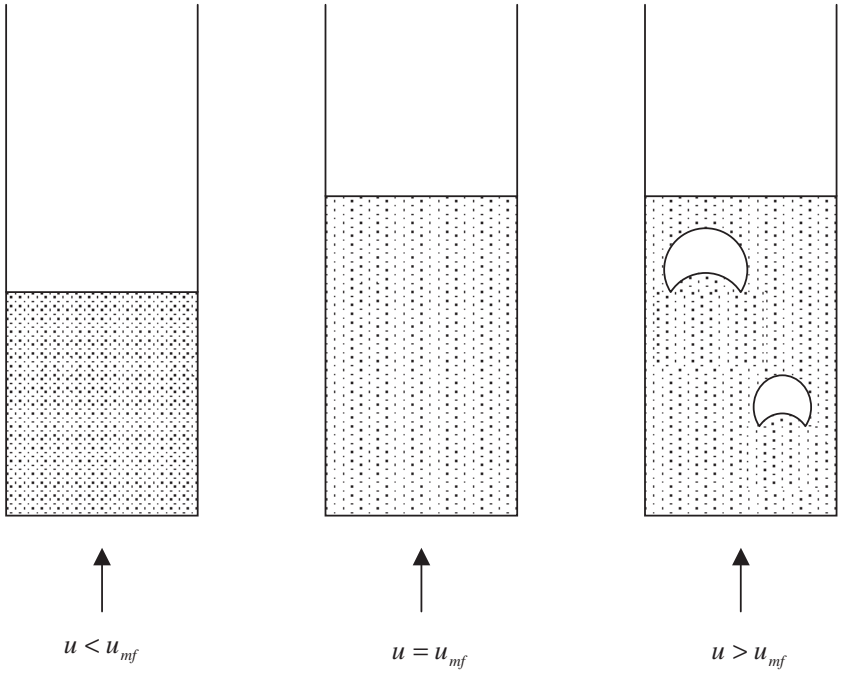

Figure 1.2 Aggregative fluidization.

Thus fluidization is a technique which enables solid particles to take on some of the properties of a fluid. For example, solids fluidized by a gas will adopt the shape of the container in which they are held and can be made to flow, under pressure, from an orifice or overflow a weir. If the wall of the bed is punctured by a series of apertures aligned vertically the fluidized solids will behave just as if the bed were filled with liquid; a stream of solids will issue from each aperture, that from the highest point in the bed will travel only a short horizontal distance whereas the stream from the lowest aperture will travel furthest. Gibilaro (2001) refers to a demonstration rig in the Department of Chemical Engineering at UCL in which a plastic toy duck buried in a bed of sand exchanges place with a brass duck on the bed surface when the bed is fluidized with air.*

It is possible to operate a fluidized bed in either batch or continuous mode. Strictly, most batch applications are in fact operated in semi-batch mode where the solids are treated as a batch but the fluidizing medium enters and leaves the bed continuously. In the case of gas-solid beds used in fermentation (see Chapter 6), the fluidizing gas is recirculated although reactants and products flow continuously. In true continuous operation the solids may be fed into a fluidized bed via screw conveyors, weigh feeders or pneumatic conveying lines and can be withdrawn from the bed via standpipes or by flowing over weirs.

Essentially aggregative fluidization is a two-phase system: there is a dense phase (sometimes referred to as the emulsion phase), which is continuous, and a discontinuous phase called the lean or bubble phase. The simplified assumption that all the gas over and above that required for minimum fluidization flows up through the bed in the form of bubbles is known as the two-phase theory. If the total volumetric flow of gas is Q then

$$Q = Q_{mf} + Q_B \tag{1.1}$$

where Q_{mf} is the volumetric flow of gas at minimum fluidization and Q_B is the volumetric flow rate of gas in the bubbles. The interstitial gas flows up through the dense phase of the bed in streamline flow. The particle Reynolds number (defined by equation 1.42) has a value between unity and about 10 for most fine particles, such as spray-dried

* I recall attempting to impress prospective undergraduates with this demonstration when I was a research student at UCL. From memory, rather than ducks, there were two plastic fish, one blue and weighted with sand and one pink. The demonstration purported to show how fluidized beds were able to change the colour of plastic fish . . . !

food powders, but increases by two or three orders of magnitude for large particles such as vegetable pieces in a fluidized bed freezer.

However, the rather idealised picture of a fluidized bed which has been described so far is not observed in all cases. There can be very different patterns of behaviour across a range of particle and fluid properties. For example, some solids are capable of being fluidized far more easily than others; Richardson (1971) suggests that a well-fluidized system is likely to result if the particles are fine, of low density, with an approximately spherical shape and narrow size distribution, and when the fluid is of high density. Although gas-solid systems normally give rise to aggregative fluidization and liquid-solid systems to particulate behaviour, in extreme cases particulate fluidization can occur with very small particles of low density which are fluidized by a dense gas at high pressure. In such cases increasing the gas velocity beyond u_{mf} results in significant bed expansion before bubbling begins and a minimum bubbling velocity u_{mb} may be defined as the gas velocity at which bubbles first appear. In the idealised two-phase theory, however, $u_{mf} = u_{mb}$.

Wilhelm and Kwauk (1948), in one of the earliest papers on fluidization, suggested that the Froude number, written for the minimum fluidizing condition, could be used to indicate the prevalent fluidization behaviour. Thus

$$Fr = \frac{u_{mf}^2}{gd} \tag{1.2}$$

where d is the mean diameter of the bed particles. Values of Fr below unity suggest particulate fluidization and values greater than unity suggest aggregative behaviour.

At velocities above those at which bubbling fluidization occurs, the nature of the contact between gas and solids changes significantly. As the gas velocity increases, especially in deep beds, the bubbles grow to the size of the bed container and push plugs of material up the bed as they rise. This condition is known as slugging, in which the bed particles stream past the slugs at the bed wall on their downward path. Beyond slugging, when the terminal falling velocity of the particles is exceeded, particles are entrained in the gas stream and considerable elutriation occurs. At this point large discrete bubbles are absent (Yerushalmi and Avidan, 1985) and the bed is said to be turbulent. Kunii and Levenspiel (1991) define a dense-phase bed as one in which there is a reasonably clearly defined bed surface, whether the fluidizing medium is gas or liquid. Further increase in the gas velocity beyond the turbulent fluidized condition leads ultimately to lean-phase fluidization and pneumatic conveying of the solids. However, if particles

which have been elutriated are recycled to the bed at a sufficiently high rate then a relatively high concentration of solids can be maintained in the bed. This is the condition of fast fluidization (Yerushalmi and Avidan, 1985).

Although the majority of food applications exploit the characteristics of either the dense-phase beds or particulate beds which have been described so far, there are food applications of two other phenomena: spouted beds and centrifugal fluidization. A spouted bed is a method of allowing intimate gas-solid contact for larger particles, with a minimum diameter of perhaps 1 or 2 mm, and a more regular circulation pattern than is observed in aggregative fluidization (Mathur and Epstein, 1974). Spouted beds are covered in more detail in the section on Other Types of Fluidization, below. In the centrifugal fluidized bed (see section below entitled Centrifugal Fluidization) particles enter a perforated horizontal cylinder which rotates inside a plenum with air blown across the outside of the cylinder and perpendicular to the axis of rotation. The perforated surface of the cylinder acts as the distributor plate and the centrifugal action keeps the particle bed in place close to the cylinder wall. Its particular advantage is that fluidization requires higher gas velocities than normal, thus allowing, for example, significant heat input to the bed at lower temperatures than would otherwise be possible.

A number of brief but comprehensive descriptions of basic fluidized bed behaviour are available (Richardson, 1971; Botterill, 1975; Couderc, 1985) which are recommended as an introduction to the subject.

Industrial applications of fluidization

The phenomena of rapid particle movement and the intimate contact between solids and at least a portion of the gas give rise to a series of characteristics of aggregative fluidization such as good mixing, near isothermal conditions and high rates of heat and mass transfer which are exploited in a wide range of unit operations.

The first significant industrial use of fluidization was in the catalytic cracking of hydrocarbons in the 1940s and arguably the most widespread use today is as a reactor for heterogeneous catalytic reactions such as the production of acrylonitrile, maleic anhydride, low-density polythene and phthalic anhydride, amongst others (Yates, 1983; Kunii and Levenspiel, 1991). Other applications have included the calcination of uranyl nitrate and radioactive aluminium nitrate wastes (Jonke *et al*., 1957), coal gasification, adsorption, drying of particulate solids (Kunii and Levenspiel, 1991), mixing (Geldart, 1992) and granulation (Sherrington and Oliver, 1981; Smith and Nienow, 1983) including the agglomeration of pharmaceutical powders (Rankell *et al*., 1964). Epstein

(2003) has reviewed the uses of liquid-fluidized beds and these include particle classification, washing, adsorption and ion exchange, flocculation, electrolytic recovery of metals, bioreactions and liquid-fluidized bed heat exchangers where the fluidized particles enhance film heat transfer coefficients and reduce the fouling of heat transfer surfaces.

Applications of fluidization in the food industry

Minimum fluidizing velocity is approximately proportional to the square of particle diameter and to the difference in density between the particles and the fluidizing medium. The majority of the applications of aggregative fluidization in the chemical processing industries involve inorganic solids of relatively high density but particle sizes at most of the order of 1 or 2 mm. Jowitt (1977) suggested that the applications of fluidization in the food industry fall into two broad categories. In the first group, food pieces are fluidized directly and because the density of food materials, particularly vegetable matter, is only a little greater than that of water it is possible to fluidize relatively large particles such as potato chips, peas, sprouts and diced vegetables even with a gas as the fluidizing medium. Jowitt's second group of applications are those where a packaged food is placed in a fluidized bed of inert solids. The heating of sealed containers in this way (i.e. cans or jars in a sterilisation operation) has a number of advantages including improved thermal economy, better control of temperature and a reduction in the consumption of process water for cooling. In a development of this idea, Rios *et al*. (1985) described a 'fluidized flotation cell' in which larger lighter objects are fluidized in a bed of denser fine particles. Optimum operation occurs at object-to-bed density ratios between 0.5 and 0.9, object-to-bed volume ratios less than 0.4 and gas velocities two or three times greater than the minimum fluidizing velocity of the fines. Outside these conditions, the objects tend either to float on the bed surface or sink. Such systems also require separation of the floating objects from the fines; this is a possible disadvantage although the authors suggest that in some cases this can be accomplished easily by simple screening.

Many of the uses of gas-solid fluidized beds in the chemical and processing industries, for example as driers, mixers, granulators and reactors, are relevant also in food processing but in addition there are a number of food-specific applications such as freezing, blanching, cooking and roasting (Jowitt, 1977; Smith, 2003) and the sterilisation of canned foods (Jowitt, 1977). Shilton and Niranjan (1993) have reviewed the uses of fluidization in food processing. In fluidized bed freezing the solids to be frozen are fluidized by refrigerated air at temperatures of –30°C or below and the particles are frozen independently and very rapidly to give a free-flowing IQF (Individually Quick Frozen) product;

in a fluidized bed drier the enthalpy of vaporisation is supplied by the fluidizing gas which is usually air, although submerged heating elements can also be used; in mixing applications the bed particles are moved rapidly by the action of rising bubbles; granulation covers those processes which produce granules or instantised products from a solution or slurry and again the heat for evaporation of the solvent is usually supplied by the fluidizing gas. A related process is fluidized bed coating where the objective is to coat particles or tablets with a solid material such as lactose but avoid particle growth by agglomeration (Vinter, 1982).

Rios *et al*. (1985) reported the use of a fluidized bed for the roasting of coffee beans, resulting in improved quality compared to traditional rotating drum methods. However, the fluidized bed technique involved increased costs and higher levels of pollution due to the rejection of hot exhaust gases. Rios and co-workers have also proposed the use of a 'whirling bed apparatus' in which a wedge placed on the gas distributor plate induces a cyclical particle motion and high-intensity mixing (Rios *et al*., 1985). Coupled with gas recycle, this experimental coffee roasting method allowed for aroma recovery and reduced energy consumption and gave an improved product quality. Roasting times were reduced from the 10–15 minutes in the conventional drum method to between 2 and 4 minutes in the whirling bed apparatus (Arjona *et al*., 1980). The blanching of vegetables with a mixture of air and water vapour in a combined fluidized bed conveyor belt system has been reported to give a reduction in energy consumption of over 20% compared to water blanching, a significant reduction in the loss of vitamin C and reduced waste water treatment costs (Rios *et al*., 1978, 1985).

Liquid fluidization is the basis of both the Oslo (or Krystal) continuous crystalliser (Mullin, 1993) which is used in the production of, for example, sugar or citric acid, and the bioreactors in which immobilised cells or enzymes are fluidized by the reactant solution (Epstein, 2003). It is used in the leaching of vegetable oils from seeds (Rios *et al*., 1985; Epstein, 2003) and in physical operations such as the washing and preparation of vegetables.

The details of food processing applications are covered in Chapters 3–7; the remainder of this chapter deals with a detailed description of fluidized bed behaviour.

Gas-solid fluidized bed behaviour

Influence of gas velocity

The relationship between bed pressure drop and superficial fluidizing velocity is shown in Figure 1.3. As the gas velocity increases, the

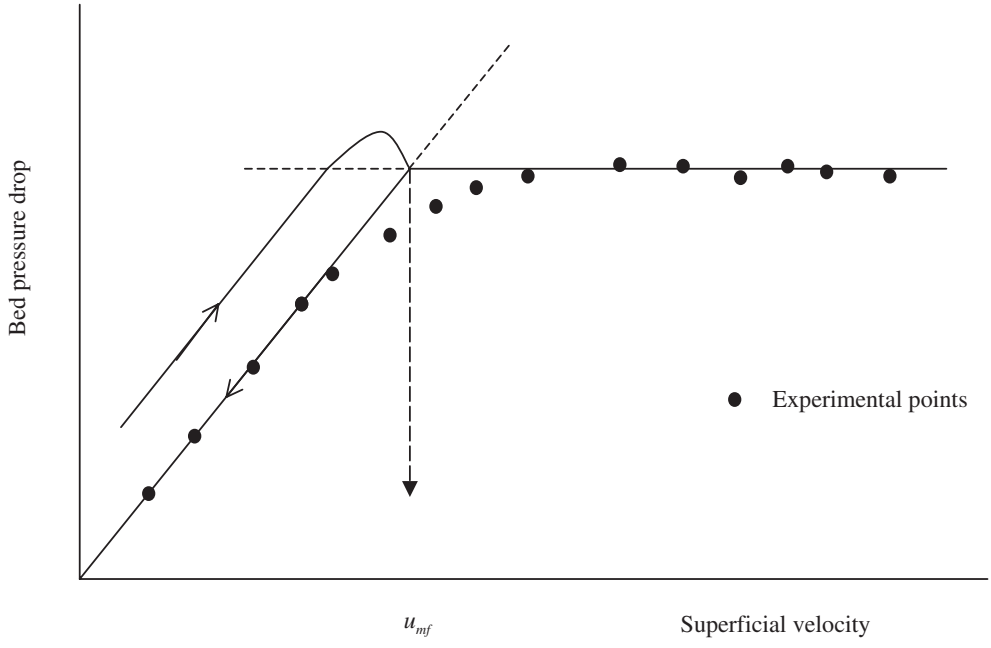

Figure 1.3 Relationship between bed pressure drop and superficial fluidizing velocity.

pressure drop increases in the fixed bed, or packed bed, region and then levels out as the bed becomes fluidized. Ideally, the pressure drop then remains constant as the weight of the particles is supported by the fluid. However, if the velocity is then reduced, marked hysteresis is observed. This is because the bed voidage remains at the minimum fluidizing value whereas with increasing gas velocity considerable vibration of the particles takes place, the voidage is lower and the pressure drop correspondingly is slightly greater. In practice, too, there will be a maximum pressure drop through which the curve passes because of particle interlocking. Also, as the velocity is reduced, the transition between the fluidized and fixed curves is gradual rather than sudden.

As the superficial gas velocity is increased beyond the minimum fluidizing velocity, a greater proportion of gas passes through the bed in the form of bubbles, the bubbles grow larger, particle movement is more rapid and there is a greater degree of 'turbulence'. Fluidizing gas velocity is the single most important variable affecting the behaviour of a bed of given particles and it is expressed usually as either:

(1) multiples of u_{mf}

e.g. $\frac{u}{u_{mf}} = 3$ implies that the gas velocity is three times that required for minimum fluidization, or as

(2) excess gas velocity, $u - u_{mf}$

e.g. $u - u_{mf} = 1.2\,\mathrm{m\,s^{-1}}$ implies that the gas velocity is $1.2\,\mathrm{m\,s^{-1}}$ *greater* than that required for minimum fluidization.

In practice, proportionately more gas flows interstitially (i.e. between the particles) as the velocity is increased than at u_{mf}. In addition, there is a limited interchange of gas between the bubble phase and the dense phase. As the gas velocity is increased further the very smallest particles are likely to be carried out of the bed in the exhaust stream. This is because at any realistic fluidizing gas velocity, the terminal falling velocity of the very smallest particles will be exceeded. The loss of bed material in this way is known as elutriation and will increase as $\frac{u}{u_{mf}}$ increases. Further increases in gas velocity result in greater elutriation and a more dilute concentration of the solids remaining in the bed. Eventually all the particles will be transported in the gas stream at the onset of pneumatic conveying.

The section above the fluidized bed surface is often referred to as the freeboard. This section may have a gradually increasing column diameter, rather like an inverted cone, which is designed to reduce the gas velocity and thus disengage gas and particles. Particles then fall back to a level where the superficial gas velocity is sufficient to support their weight.

Geldart's classification

Fluidized bed behaviour is affected not only by gas velocity but also by particle size and density. Based upon observations of fluidized bed behaviour in air at ambient conditions and at velocities below $\frac{u}{u_{mf}} = 10$, Geldart (1973) suggested classifying fluidized particles into four groups: C (cohesive), A (aeratable), B (sand-like) and D (spoutable). This classification is shown diagrammatically in Figure 1.4 in the form of a plot of the density difference between particle and fluid against mean particle size.

Group A particles are typically between $20\,\mu$m and $100\,\mu$m in diameter with a particle density less than $1400\,\mathrm{kg\,m^{-3}}$. These particles exhibit considerable bed expansion as the fluidizing velocity increases and collapse only slowly as the velocity is decreased. In other words, they tend to retain the fluidizing gas. The bubbles are limited in size and frequently split up and coalesce as they rise through the bed. On the other hand, the larger and denser group B particles ($40–500\,\mu$m, particle density in the range $1400–4000\,\mathrm{kg\,m^{-3}}$) form freely bubbling fluidized beds at or slightly above the minimum fluidizing velocity. Small

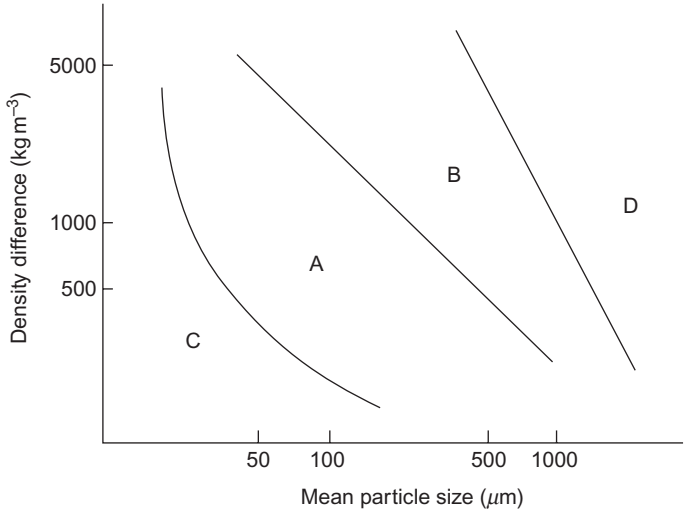

Figure 1.4 Geldart's classification.

bubbles form at the distributor and grow by vertical coalescence as they rise up the bed. The increase in bubble size is approximately linear with increasing excess gas velocity and height above the distributor plate and size is limited only by the diameter of the bed. Vigorous bubbling brings about considerable solids mixing. This is the classic fluidized bed behaviour; group B particles can be defined by

$$(\rho_s - \rho_f)^{1.17} \geq 9.06 \times 10^5 \qquad 1.3$$

Group C, with particle diameters below $30\,\mu$m, consists of cohesive powders which display a tendency to agglomerate and are very difficult to fluidize; the forces between particles are greater than the hydrodynamic force which is exerted on the particle by the fluidizing gas. In small-diameter beds the particles tend to move upwards as a solid plug. As the bed diameter increases, relatively little bubbling is observed and instead the gas passes up through the bed in a series of channels. This group is characteristic of a number of food materials such as flour or very fine spray-dried particles. Geldart (1992) suggested that these powders can be identified by measuring both the tapped and aerated bulk densities. If the ratio of the two exceeds a value of 1.4 then the particles are likely to be group C.

Large particles with a mean diameter greater than $600\,\mu$m and a density above $4000\,\text{kg m}^{-3}$ are classed as group D and whereas in Geldart B beds the bubbles tend to rise faster than the gas in the dense phase, the reverse is true of bubbles in Geldart D particle beds. Bubbles tend to coalesce horizontally rather than vertically and reach a large

size. The resulting solids mixing is poorer than in Geldart B beds. Slugging occurs if the bubble size approaches the bed diameter and large Geldart D beds are prone to spouting (see section on Spouted Beds below). Such particles display very little bed expansion and generally give unstable fluidization; channelling of the gas is prevalent. Food examples include seeds and vegetables pieces. Group D particles can be defined by

$$(\rho_s - \rho_f)d^2 \geq 10^9 \qquad 1.4$$

Bubbles and particle movement

Bubble formation at the distributor

The growth of a typical bubble at a small aperture in the distributor plate was described by Zenz (1971) and is illustrated in Figure 1.5 which shows the changes in the interface between the fluidizing gas entering the bed through an aperture in the distributor plate and the dense phase of the bed. The velocity u of gas passing through the aperture and into the bed will be greater than the minimum fluidizing velocity of the bed particles u_{mf} by at least an order of magnitude and therefore will be sufficient to lift the interface between gas and bed particles into the position shown in Figure 1.5b. As the void grows (Figure 1.5c), the mean velocity of gas passing through the interface will decrease by a factor equal to the ratio of the aperture area to the area of the interface. Zenz suggested that if this mean velocity is still greater than u_{mf} then the interface will remain stable and the void will grow still further, as in Figure 1.5c. At some point the void is large enough that the velocity through the interface decreases to the value of u_{mf} and therefore the void reaches its maximum size. The pressure exerted by the fluidized particles is greater at the base of the void than at its uppermost point, due simply to the depth of 'fluid'; that is, the depth of the dense phase. Thus the interface collapses at the base of the void, cutting off the incoming gas into a bubble with a more stable and near-spherical shape. A new interface between the inlet gas and bed particles is then formed and the process is continually repeated. Consequently the volumetric flow rate of gas and the minimum fluidizing velocity of the bed particles influence the initial size of bubbles formed at the distributor (Zenz, 1971).

Bubble growth and bubble shape

The bubbles in a fluidized bed have a distinct shape and there is a distinct boundary between the gas in the bubble and the

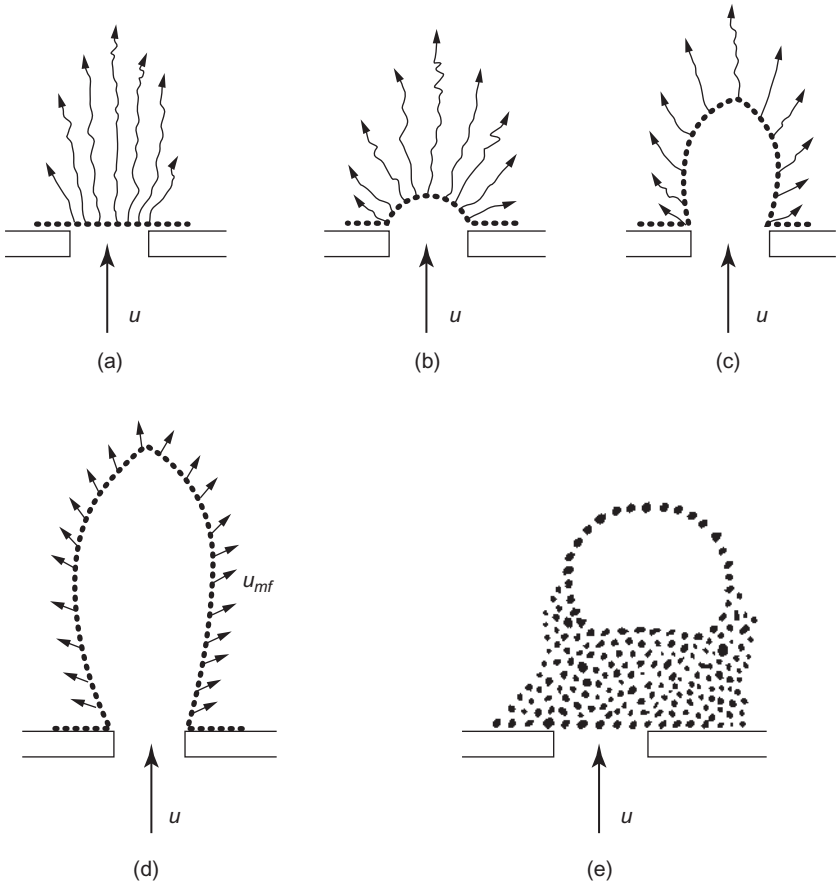

Figure 1.5 Bubble formation at the distributor. Reprinted from Davidson, J.F. and Harrison, D., Fluidization, Academic Press, 1971, with permission from Elsevier.

surrounding dense phase although the boundary tends to oscillate. A single bubble, rising in a bed where the bubble diameter is much less than the bed diameter, is essentially spherical but with a slight indentation at the base. However, the shape can be influenced and distorted by close proximity to either the bed walls and or submerged surfaces such as heat transfer coils or the nozzles used for injecting liquid in some applications. Both the shape and size are affected when the bubble diameter becomes greater than about half the bed diameter. Rowe (1971) suggested that the minimum size of a bubble is 1–2 orders of magnitude greater than the size of the particles in the bed, which implies a minimum diameter of about 0.005 m in fine powders and 0.10 m in beds of coarse particles with a diameter of several mm.

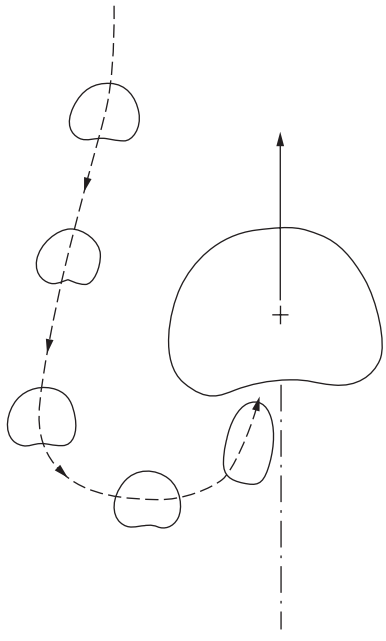

Figure 1.6 Coalescence of bubbles. Reprinted from Davidson, J.F. and Harrison, D., Fluidization, Academic Press, 1971, with permission from Elsevier.

Bubbles grow as they rise through the bed and, although there is some interchange of gas between bubbles and the dense phase, growth is due mainly to coalescence. Small bubbles are overtaken by larger ones, which rise at a greater velocity, and coalescence takes place at the base of the larger bubble, as in Figure 1.6. Vertical indentations often develop downwards from the roof of the bubble which then grow to split the bubble in half vertically but growth by coalescence is far more significant than any size reduction. As they grow, the size of the indentation at the base of a bubble increases and they take on the characteristic kidney-shape shown in Figure 1.7. The total volumetric flow rate of gas in the bubble phase is approximately constant and consequently the number of bubbles at any bed cross-section decreases with bed height.

As Rowe (1971) has shown in a series of experiments using a tracer gas in a two-dimensional bed, the interstitial gas in a bubbling bed enters the base of a bubble and emerges through the bubble roof, resulting in some interchange of gas between the dense and bubble phases. However, if the rise velocity of a bubble exceeds u_{mf}, on leaving the bubble the gas is swept down the side of the bubble and re-enters at the base. Thus an approximately spherical cloud of gas surrounds the bubble and moves with it up through the bed. In other words, there are in effect two phases formed within the bubble gas. This

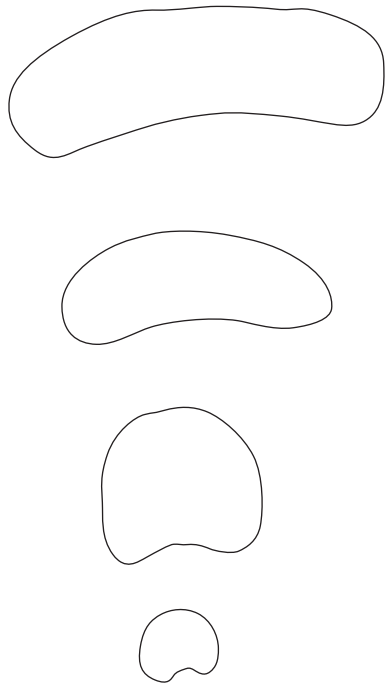

Figure 1.7 Characteristic bubble shapes.

phenomenon has significant consequences for the degree of gas interchange in aggregative fluidization and much effort has been expended in modelling it in terms of the performance of fluidized bed chemical reactors. As yet this appears to have little relevance to the food applications of fluidization although it may become significant in fluidized bed fermentation when this operation is better understood.

Minimum bubbling velocity

Minimum bubbling velocity u_{mb} is defined as the gas velocity at which bubbles first appear in aggregative fluidization. For coarse uniformly-sized particles, for example those in Geldart group B, it is usually the case that $u_{mb} \cong u_{mf}$. However, very fine non-uniformly sized particles such as those in group A exhibit smooth bed expansion and no bubbling until a gas velocity considerably in excess of the minimum fluidizing velocity is reached. The ratio $\frac{u_{mb}}{u_{mf}}$, which indicates the degree to which bed expansion occurs, is a strong function of mean particle size and increases to values greater than unity, and perhaps as high as 2 or 3, as the particle size falls below about 100 μm. According

to Abrahamson and Geldart (1980), this ratio depends particularly on the fraction of fines below 45 μm. They measured the minimum bubbling velocity for a wide range of fine particles in the range 20–72 μm and proposed the following correlation to predict $\frac{u_{mb}}{u_{mf}}$

$$\frac{u_{mb}}{u_{mf}} = \frac{2300\rho_f^{0.13}\mu^{0.52}\exp(0.72\omega_{45})}{d^{0.8}(\rho_s - \rho_f)^{0.93}} \quad 1.5$$

where the mean particle size d, gas viscosity μ and the gas and solid densities ρ_f and ρ_s respectively are quoted in SI units and ω_{45} is the mass fraction of fines less than 45 μm in diameter.

Bubble rise velocity

The phenomenon of a gas bubble rising in a fluidized bed is similar to that of a gas bubble rising in a liquid; bubbles rise through the bed at a constant velocity for a given size, this velocity being proportional to bubble diameter. The general relationship for a single bubble is of the form

$$u_{SB} = k\sqrt{gd_B} \quad 1.6$$

where, using SI units, it is usually assumed that k has a value of approximately 0.67 although for fine particles this underestimates velocity somewhat and Botterill (1975) suggests that k should be about 50% higher. Kunii and Levenspiel (1991) suggest k = 0.71 and that, based on a theory due to Davidson and Harrison (1963), the rise velocity for bubbles in a bubbling bed u_B is equal to the rise velocity of a single bubble plus the excess gas velocity, hence

$$u_B = u_{SB} + (u - u_{mf}) \quad 1.7$$

To give an example of likely bubble rise velocities, take a fine powder with a mean particle diameter of 200 μm and a particle density of 1500 kg m^{-3}. The Ergun equation (see equation 1.48) gives the minimum fluidizing velocity as u_{mf} = 0.05 m s^{-1}. Now calculating u_{SB}, the rise velocity of a single bubble, from equation 1.6 with k = 0.71, and the rise velocity in a bubbling bed from equation 1.7, gives the data in Table 1.1. Combinations of two fluidizing gas velocities and two bubble diameters have been assumed. This calculation suggests that in a bubbling bed of the given powder, bubbles are likely to rise at velocities in the approximate range 0.5–1 m s^{-1}.

Table 1.1 Calculated rise velocity of bubbles.

Velocity ($m\,s^{-1}$)	$\frac{u}{u_{mf}} = 3$		$\frac{u}{u_{mf}} = 10$	
	$d_B = 0.025\,m$	$d_B = 0.075\,m$	$d_B = 0.025\,m$	$d_B = 0.075\,m$
u	0.15	0.15	0.50	0.50
$(u - u_{mf})$	0.10	0.10	0.45	0.45
u_{SB}	0.35	0.61	0.35	0.61
u_B	0.45	0.71	0.80	1.06

Particle movement due to bubble motion

Particle mixing in a fluidized bed is brought about solely by the movement of bubbles. The space between the indented base of a bubble and the bubble sphere is known as the wake and is occupied by particles. As a bubble rises in the bed (Figure 1.8) it carries with it this wake of particles and then draws up a spout of particles behind it. The wake grows as the bubble rises but a proportion of the wake may also be shed before the bubble reaches the bed surface. Thus the wake fraction, the fraction of the bubble sphere occupied by the wake, varies with time as a bubble rises to the bed surface. The wake fraction also varies with particle size in the approximate range 0.15–0.4 for a variety of (non-food) particles in the size range 60–600 μm; larger wake fractions have been observed with smaller particles but there is no clear relationship. Growth and shedding of the wake may be repeated several times in the life of a single bubble. Overall, a quantity of particles equal to one bubble volume is moved through a distance of 1.5 bubble diameters by a single rising bubble. Because of the large numbers of bubbles present in a fluidized bed, the particle mixing pattern is highly complex and extremely rapid.

Based upon these observations, Rowe (1977) derived an expression for the average particle circulation time t around a bed in terms of excess gas velocity and bed height at minimum fluidization

$$t = \frac{H_{mf}}{0.6(u - u_{mf})} \tag{1.8}$$

Although this expression may not accurately predict circulation time, and in any case particles do not follow a simple predetermined circuit around the bed, it serves to illustrate the significance of the excess gas velocity in determining particle mixing rates. The excess gas flow rate, proportional to the excess gas velocity, is essentially the bubble flow rate. A greater bubble flow generates more bubbles and therefore

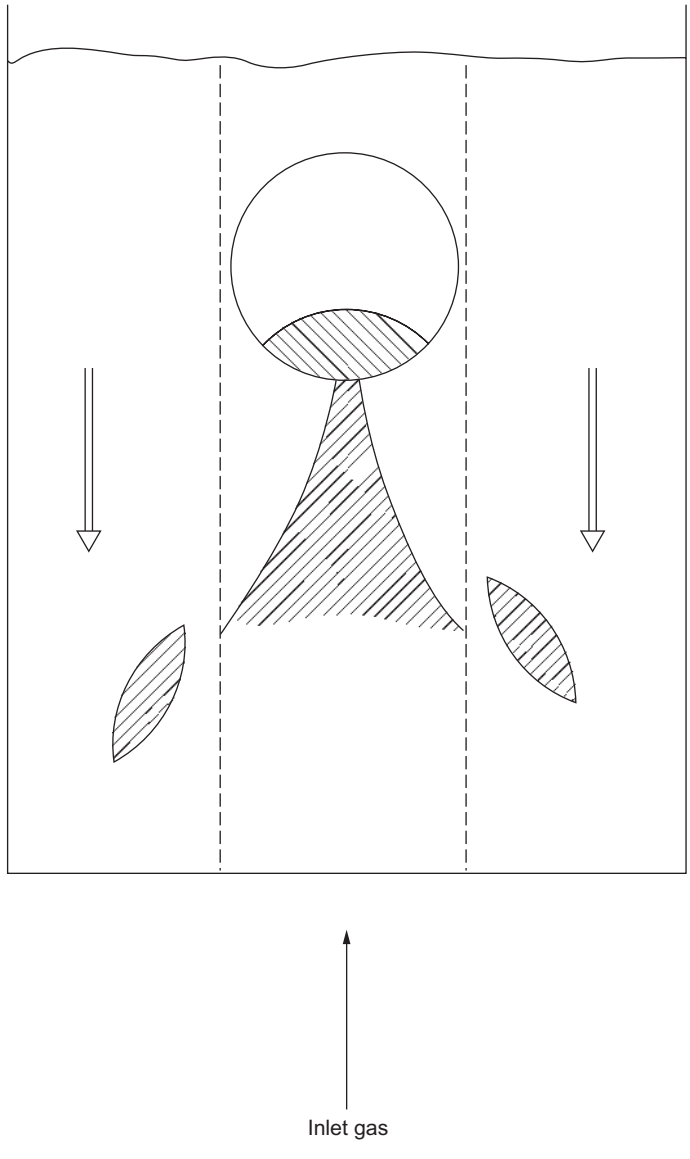

Figure 1.8 Mechanism of particle mixing in a fluidized bed. From Smith, P.G., Introduction to food process engineering, Kluwer, 2003, figure 13.15. With kind permission of Springer Science and Business Media.

greater particle movement in unit time and more rapid particle circulation. The rapid particle movement in a fluidized bed leads to its use in particle mixing but is also essential in all other applications of fluidization. However, the mixing mechanism is opposed by segregation, where the concentration of one component increases at the bottom of the bed. Particle size has only a slight influence upon segregation

(unlike in mechanical mixers). However, segregation increases markedly with the difference in density between two components. When the density ratio reaches a value of about 7, almost no mixing occurs in a fluidized bed. Three main mechanisms can be identified by which particles move in a bed and thus bring about either mixing or segregation:

- particles rising in bubble wakes
- large, dense particles falling through bubbles
- small, dense particles percolating downwards through the interstices of the dense phase of the bed.

Particle mixing is covered at greater length in Chapter 2.

Distributor plate design

A fluidized bed requires a distributor plate which supports the bed when it is not fluidized, prevents particles from passing through and promotes uniform fluidization by distributing the fluidizing medium evenly. In aggregative fluidization the nature of the distributor plate significantly influences the number and size of bubbles formed. A wide variety of distributors can be used including porous or sintered plates, manufactured from either ceramic or metal, layers of wire mesh, drilled plates, nozzles, tuyeres, bubble caps or pipe grids. Whatever the structure of the distributor plate, it must have many small orifices to allow gas to be injected at a multitude of points; a coarse distributor results in high gas rates at localised points and thus channelling in the bed (Richardson, 1971). Botterill (1975) summarised the requirements of a distributor which should:

(1) promote uniform and stable fluidization
(2) minimise the attrition of bed particles
(3) minimise erosion damage, and
(4) prevent the flow-back of bed material during normal operation and on interruption of fluidization when the bed is shut down.

Generally the pressure drop across the plate should be high to promote even gas distribution and is usually some fraction of the pressure drop across the fluidized bed; porous distributors tend to have much higher pressure drops than other types of plate.

Porous or sintered plates are the ideal and are used in small-scale studies of fluidized bed behaviour (Kunii and Levenspiel, 1991) and form a highly expanded unstable gas-solid dispersion directly above the distributor which rapidly divides into a large number of small bubbles plus an emulsion phase. Bubbles grow rapidly thereafter by coalescence. Kunii and Levenspiel (1991) also suggest that other

materials offer similar properties to porous plates, including filter cloths, compressed fibres, compacted wire plates and even thin beds of small particles. According to Richardson (1971), porous plates are best in terms of the quality of fluidization but become expensive for large beds and also suffer from poor mechanical strength. Other disadvantages include the high pressure drop across the plate leading to increased power requirements and operating costs; sensitivity to thermal stresses; and blockage of the plate by fine particles or by the products of corrosion.

Perforated plate distributors are widely used in industry because they are cheap and relatively easy to manufacture. Simple perforated plate-type distributors suffer from particles passing back through to the plenum despite mean gas velocities well above the settling velocity for the particles. This is because of imbalances in gas flow between the orifices, which is difficult to eliminate. Hence, such plates take the form of either a layer of mesh sandwiched between two perforated plates or two staggered perforated plates without a mesh screen (Kunii and Levenspiel, 1991). However, these structures often lack rigidity and need to be reinforced or sometimes curved (concave to the bed) to withstand heavy loads. The diameter of the orifices in a perforated plate distributor varies from 1 or 2 mm in small beds used for research or very small-scale production to 50 mm in very large chemical reactors. Most food applications are likely to use apertures of intermediate size.

Perforated plate distributors cannot be used under severe operating conditions, such as high temperature or a highly reactive or corrosive environment. This is unlikely to be a disadvantage for food applications of fluidization, but in such circumstances tuyeres, nozzles or bubble caps are used. There is a very wide variety of designs (Kunii and Levenspiel, 1991) from open nozzles to complex bubble caps. The latter have small orifices around the periphery of a cap which rises or falls depending on the balance between the pressure of gas below and the back-pressure from above. The use of bubble caps can prevent the back-flow of solids (Botterill, 1975) and they may be designed to allow stagnant defluidized solids to lie between the caps, for example to provide thermal insulation for the protection of the distributor in high temperature processes. However, the potential disadvantages include the settling of particles between tuyeres or nozzles, the need to ensure that the incoming gas is free of fine particles which may clog the distributor, and the considerable expense of construction.

The pressure drop across the plate ΔP_d should be high to promote even gas distribution and stable fluidization and is usually some fraction of bed pressure drop ΔP although Kunii and Levenspiel (1991) point out that an excessive ΔP_d has the disadvantage of significantly

increased power consumption and construction costs for the compressor. The pressure drop across a porous plate distributor increases in proportion to the superficial gas velocity whilst that for a perforated plate or a tuyere or nozzle type increases in proportion to the square of the gas velocity. It is important therefore to design for the minimum pressure drop that gives acceptable fluidization quality.

For a shallow bed, the pressure drop across the distributor should be of the same order as the bed pressure drop (Richardson, 1971). Hiby (1964) suggested $\frac{\Delta P_d}{\Delta P} = 0.15$ at low gas velocities of $\frac{u}{u_{mf}} \cong 1-2$ and $\frac{\Delta P_d}{\Delta P} = 0.015$ for $\frac{u}{u_{mf}} \gg 2$. This stability of fluidization with a relatively low plate pressure drop at higher gas velocities is because the fluidized bed behaves effectively as its own distributor and explains why ΔP_d can be a smaller fraction of ΔP with deeper beds. Siegel (1976) proposed a minimum value of 0.14 for $\frac{\Delta P_d}{\Delta P}$ whilst Shi and Fan (1984) suggested the same figure for porous plates and a value of 0.07 for perforated plates.

Characterisation of particulate solids

A knowledge of the minimum fluidizing velocity of fluidized solids is essential for the effective design and operation of fluidized beds which may be used for mixing, drying, freezing or other unit operations. The available predictive equations for minimum fluidizing velocity require a knowledge of the size, and sometimes the shape, of particles as well as the properties which characterise the particle bed. Some models require a knowledge of the terminal falling velocity of the particles. Therefore it is appropriate at this point to outline the ways in which particulate solids can be characterised and their bulk behaviour described, and in addition to give an elementary coverage of the interaction of a particle with a fluid before proceeding to the prediction of minimum fluidizing velocity.

Particle size distribution

Any sample of particulate food solids, whether naturally occurring or the result of a manufacturing process, will contain a distribution of particle sizes. However, despite the fact that the existence of a distribution of sizes can affect fluidized bed behaviour very significantly, predictive models, especially those which have been proposed for the prediction of minimum fluidizing velocity, usually require a single

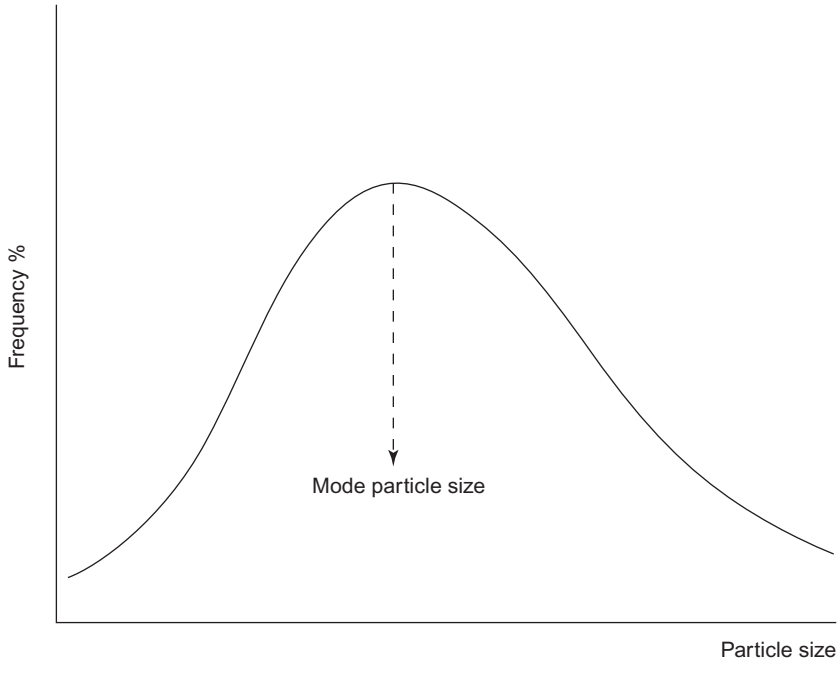

Figure 1.9 Frequency distribution curve.

value of particle size. Two expressions of 'average' size can be obtained from particle size distribution curves (Allen, 1981; Smith, 2003). The mode size is the most frequently occurring size and is represented by the peak of the frequency distribution curve, i.e. a plot of the frequency with which a given particle size occurs against that size (Figure 1.9). The frequency distribution curve also shows clearly the overall shape of a particle size distribution and the presence of very large or very small particles. Particle size data can also be plotted as a cumulative distribution in which either the cumulative percentage undersize or cumulative percentage oversize is plotted against size. These two curves are mirror images of each other (Figure 1.10) and the median particle size is the 50% point on either of the cumulative curves, which in turn must be the intersection of the undersize and oversize curves. In other words, it is that particle size which cuts the area under the frequency distribution curve in half. Although each of these quantities gives an indication of the average size, neither takes account of the spread of the distribution and it is possible to obtain the same mode or median with either a very narrow or a very wide distribution. These difficulties can be overcome by a using a carefully defined mean particle size.

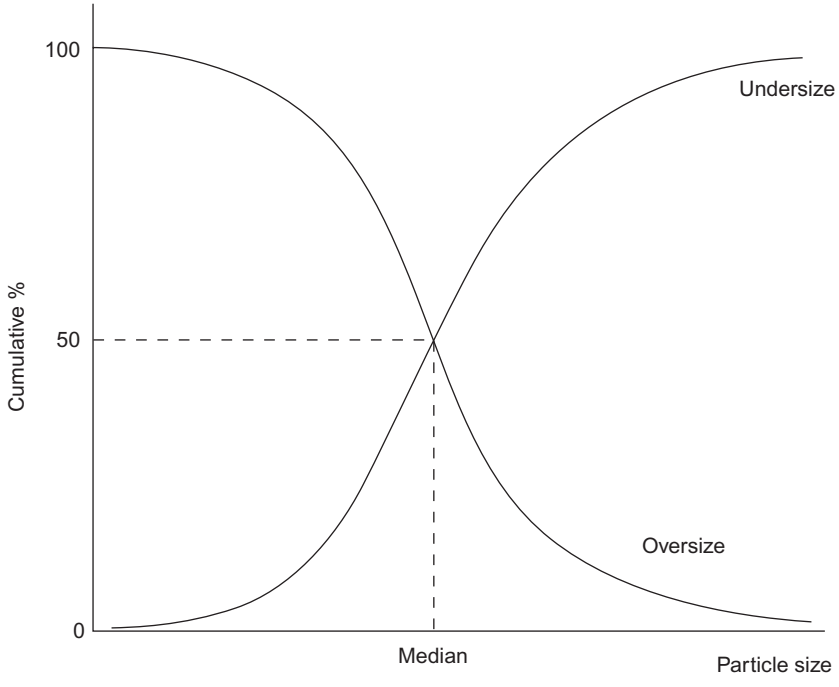

Figure 1.10 Cumulative percentage undersize and oversize curve.

Mean particle size

The characteristics of a particle size distribution can be defined as the total number, total length, total surface area and total volume of the particles. A distribution of particle sizes can be represented by a set of uniformly-sized particles which retains two characteristics of the original distribution. The mean particle size of a distribution is then equal to the size of the uniform particles with respect to the two characteristics. Thus, for the definition of mean particle size, Mugele and Evans (1951) proposed

$$x_{q,p}^{q-p} = \frac{\int_{x_l}^{x_u} x^q \frac{dN}{dx} dx}{\int_{x_l}^{x_u} x^p \frac{dN}{dx} dx} \tag{1.9}$$

where N is the number of particles of size x and p and q are parameters representing the characteristics of a distribution; x_l and x_u are the lower and upper limits of the size distribution respectively. Values of 0 for number, 1 for length, 2 for area and 3 for volume are assigned to the parameters p and q. Most methods of determining particle size

generate data in the form of the number of particles within a given size band. The mean size is then obtained by summing over all the band widths and the model becomes

$$x_{q,p}^{q-p} = \frac{\sum(x^q N)}{\sum(x^p N)} \tag{1.10}$$

Substituting all the possible combinations of characteristics, i.e. values of p and q, into equation 1.10 gives rise to a number of different definitions of the mean size of a distribution. At minimum fluidization the drag force acting on a particle due to the flow of fluidizing gas over the particle is balanced by the net weight of the particle. The former is a function of surface area and the latter is proportional to particle volume. Consequently the surface-volume mean diameter, with $p = 2$ and $q = 3$, is the most appropriate particle size to use in expressions for minimum fluidizing velocity. It is defined by equation 1.11

$$x_{3,2} = \frac{\sum(x^3 N)}{\sum(x^2 N)} \tag{1.11}$$

Of the many ways of measuring or deducing the size of particles, sieving remains one of the easiest and cheapest and is very widely used. Although time consuming, it is the only method which gives a mass distribution and the only method which can be used for a reasonably large sample of particles which are not in suspension. A sieve analysis is carried out by placing a sample on the coarsest of a set of standard sieves made from woven wire. Below this sieve the other sieves are arranged in order of decreasing aperture size. The sample is then shaken for a fixed period of time, and the material on each sieve collected and weighed. For particularly fine or cohesive powders, air swept sieving can be used in which an upward flow of air from a rotating arm underneath the mesh prevents blockage of the sieve apertures.

The definition of the surface-volume mean diameter given by equation 1.11 must be modified for use with data from a sieve analysis. By assuming that the shape and density of the particles are constant for all size fractions, a number distribution can be transformed to a mass distribution (Smith, 2003) and therefore the surface-volume diameter becomes

$$x_{3,2} = \frac{1}{\sum\left(\frac{\omega}{x}\right)} \tag{1.12}$$

where ω is the mass fraction of particles of size x. The surface-volume mean is also known as the Sauter mean diameter or the harmonic mean diameter.

Particle shape

Relatively little appears to be known about the influence of shape on the behaviour of particulate solids and it is notoriously difficult to measure. Whilst a sphere may be characterised uniquely by its diameter and a cube by the length of a side, few natural or manufactured food particles are truly spherical or cubic. For irregular particles, or for regular but non-spherical particles, an equivalent spherical diameter d_e can be defined as the diameter of a sphere with the same volume V as the original particle. Thus

$$V = \frac{\pi}{6} d_e^3 \tag{1.13}$$

More commonly, a generalised volume shape factor K' is used to relate particle volume V to the cube of particle size

$$V = K' x^3 \tag{1.14}$$

The following has been suggested (Richardson and Zaki, 1954; Richardson, 1971) for fluidized cubes and cylinders

$$K'' = \frac{\pi}{6} \frac{d_s^3}{d_p^3} \tag{1.15}$$

where d_s is the diameter of a sphere with the same surface area as the particle and d_p is the diameter of a circle having an area equal to the projected area of the particle in its most stable position.

The sphericity ϕ of a particle, where the respective surface areas of the particle and an equivalent sphere are compared, has also been found to be useful in characterising shape. Thus

$$\phi = \frac{\text{surface area of sphere of equal volume to particle}}{\text{surface area of particle}} \tag{1.16}$$

For non-spherical particles, values of sphericity lie in the range $0 < \phi < 1$. Thus, the effective particle diameter for fluidization purposes is the product of the surface-volume mean diameter and the sphericity (Kunii and Levenspiel, 1991). The sphericity of regular-shaped particles can be deduced by geometry whilst the sphericity of irregular-shaped

particles has to be determined by experiment. This is achieved by passing gas upwards through a packed bed of the particles at gas velocities below the minimum fluidizing velocity and measuring the packed bed interparticle voidage and frictional pressure drop. Kunii and Levenspiel (1991) suggest inserting these, and other appropriate values, into the Ergun equation (see equation 1.48) to obtain an average value for the sphericity. This procedure was used by Mishra *et al.* (1982) to estimate the sphericity for packed beds of grated yeast pellets.

Bulk particle properties

Expressions for minimum fluidizing velocity can be derived by examining the relationship between the velocity of a fluid passing through a packed bed of particles and the resultant pressure drop across the bed. Consequently it is necessary to define a number of bulk particle properties which influence fluidized bed behaviour.

The solids density ρ_s is the density of the solid material from which the particle is made and excludes any pore spaces within the particle. It can be measured using a specific gravity bottle and a liquid in which the particle does not dissolve. The envelope density of a particle is that which would be measured if an envelope covered the external particle surface, i.e. it is equal to the particle mass divided by the external volume. In most analyses the envelope and solids densities are assumed to be equivalent. The bulk density of a powder ρ_B is the effective density of the particle bed defined by

$$\rho_B = \frac{\text{mass of solids}}{\text{total bed volume}} \tag{1.17}$$

The bulk density will be considerably smaller than the solids density because the bed volume includes the volume of the spaces between particles.

Intraparticle porosity refers to the fraction of the particle volume which is occupied by internal pores; most manufactured food particles are porous. However, it is important to distinguish this quantity from bed voidage. The interparticle voidage ε is the fraction of the packed bed occupied by the void spaces between particles and is defined as

$$\varepsilon = \frac{\text{void volume}}{\text{total bed volume}} \tag{1.18}$$

This can be written as

$$\varepsilon = \frac{\text{total bed volume} - \text{particle volume}}{\text{total bed volume}} \tag{1.19}$$

or

$$\varepsilon = 1 - \frac{\text{particle volume}}{\text{total bed volume}} \tag{1.20}$$

Volume is inversely proportional to density and therefore equation 1.20 becomes

$$\varepsilon = 1 - \left(\frac{\rho_B}{\rho_s} \right) \tag{1.21}$$

The specific surface S is the external surface area of a particle per unit particle volume and for a sphere this is equal to $\frac{6}{d}$. The total surface area of a porous particle, including that of the internal pore spaces, can be measured by gas adsorption techniques and may be of the order of several hundred square metres per gram of material.

Terminal falling velocity and particle drag coefficient

Figure 1.11 represents the cross-section through a spherical particle over which an ideal non-viscous fluid flows. The fluid is at rest at points 1 and 3 but the fluid velocity is a maximum at points 2 and 4. There is a corresponding decrease in pressure from point 1 to point 2 and from 1 to 4. However, the pressure rises to a maximum again at point 3. If the ideal fluid is replaced with a real viscous fluid then, as the pressure increases towards point 3, the boundary layer next to the particle surface becomes thicker and then separates from the surface as in Figure 1.12. This separation of the boundary layer gives rise to

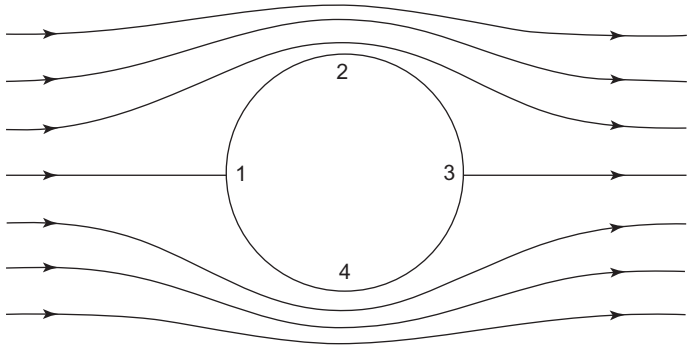

Figure 1.11 Fluid flow over a spherical particle. From Smith, P.G., Introduction to food process engineering, Kluwer, 2003, figure 13.3. With kind permission of Springer Science and Business Media.

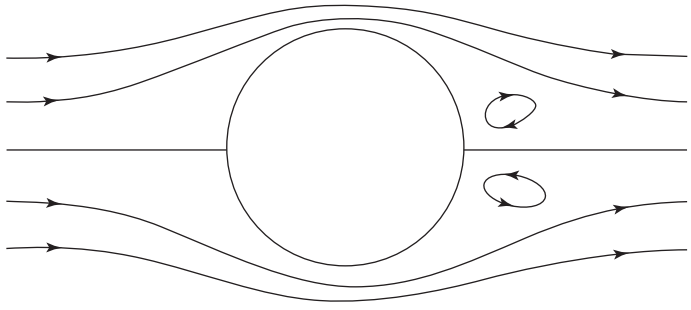

Figure 1.12 Separation of the boundary layer. From Smith, P.G., Introduction to food process engineering, Kluwer, 2003, figure 13.4. With kind permission of Springer Science and Business Media.

turbulent eddies within which energy is dissipated and which creates a force on the particle known as form drag. The total force acting on the particle because of the fluid flow is then the sum of form drag and the viscous drag over the surface.

A particle falling from rest, through a fluid, under gravity, will accelerate until it reaches a constant velocity known as the terminal falling velocity u_t. This velocity can be determined by balancing the product of particle mass and acceleration, the particle weight (mg) which pulls the particle down under gravity, the upthrust due to the fluid displaced as the particle falls ($m'g$) and the drag force (F) acting against the particle weight. Therefore

$$mg - m'g - F = m\frac{du}{dt} \tag{1.22}$$

At its terminal falling velocity the particle no longer accelerates and $\frac{du}{dt} = 0$. Substituting for this condition, for the mass (m) of a particle of diameter d and density ρ_s and for the mass of displaced fluid (m') of density ρ_f the drag force becomes

$$F = \frac{\pi}{6} g(\rho_s - \rho_f) d^3 \tag{1.23}$$

Stokes (1851) first showed that the drag force F on a sphere was given by

$$F = 3\pi d\mu u \tag{1.24}$$

where u is the relative velocity between the sphere and the fluid. Thus

$$3\pi d\mu u = \frac{\pi}{6} g(\rho_s - \rho_f) d^3 \tag{1.25}$$

and, putting $u = u_t$, the terminal falling velocity becomes

$$u_t = \frac{g(\rho_s - \rho_f) d^2}{18\mu} \tag{1.26}$$

This is Stokes' law which is valid in the particle Reynolds number range $10^{-4} < Re < 0.20$ where the Reynolds number is defined by

$$Re = \frac{\rho_f u_t d}{\mu} \tag{1.27}$$

and assumes that the particle is a single smooth, rigid sphere falling in a homogeneous fluid, that it is unaffected by the presence of any other particles and that the walls of the vessel do not exert a retarding effect on the particle.

A particle drag coefficient c_D can now be defined as the drag force divided by the product of the dynamic pressure acting on the particle (i.e. the velocity head expressed as an absolute pressure) and the cross-sectional area of the particle. This definition is analogous to that of a friction factor in conventional fluid flow. Hence

$$c_D = \frac{F}{\frac{\pi d^2}{4} \frac{\rho_f u^2}{2}} \tag{1.28}$$

On substituting for the drag force from equation 1.24, this gives

$$c_D = \frac{24}{Re} \tag{1.29}$$

for the Stokes region.

At Reynolds numbers beyond the Stokes region the boundary layer separates from the particle surface at a point just forward of the centre line of the sphere. A wake is formed containing vortices which results in larger frictional losses and a significantly increased drag force. This is known as the transition region ($0.20 < Re < 500$) where no analytical solution for the drag force is possible and empirical equations must be used to describe the relationship between drag coefficient and Reynolds number. One of the most convenient and widely used of these is that due to Schiller and Naumann (1933)

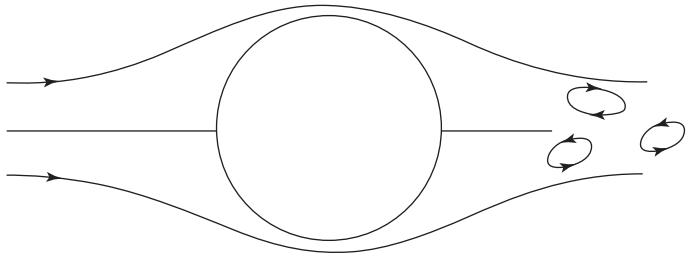

Figure 1.13 Vortex shedding. From Smith, P.G., Introduction to food process engineering, Kluwer, 2003, figure 13.4. With kind permission of Springer Science and Business Media.

$$c_D = \frac{24}{Re}(1 + 0.15Re^{0.687}) \tag{1.30}$$

As the Reynolds number increases further, vortex shedding takes place (Figure 1.13) in what is known as the Newton region, in the range $500 < Re < 2 \times 10^5$, where the drag coefficient has a value of approximately 0.44. Consequently equation 1.28 gives the drag force as

$$F = 0.055\pi d^2 \rho_f u^2 \tag{1.31}$$

which, on substitution into equation 1.23, gives the terminal falling velocity as

$$u_t = 1.74\sqrt{\frac{dg(\rho_s - \rho_f)}{\rho_f}} \tag{1.32}$$

At still greater Reynolds numbers the boundary layer itself becomes turbulent and separation occurs at the rear of the sphere and closer to the particle. In this fully turbulent region, beyond $Re = 2 \times 10^5$, the drag coefficient falls further to a value of about 0.10.

Minimum fluidizing velocity in aggregative fluidization

The superficial velocity of gas in a fluidized bed, relative to the minimum fluidizing velocity, is the quantity which has the greatest influence on the behaviour of a given particle bed. Consequently, a knowledge of minimum fluidizing velocity is vital to the operation of fluidized beds and much research effort has been expended in attempting to predict it.

Voidage and pressure drop at incipient fluidization

At the point of incipient fluidization the drag force exerted on a particle is equal to its net weight. For the whole particle bed the drag force can be equated to the product of bed pressure drop ΔP and bed cross-sectional area A. The net bed weight is then the product of bed volume, net density, the fraction of the bed $(1 - \varepsilon)$ which is occupied by particles and the acceleration due to gravity. Thus, at minimum fluidizing velocity

$$\Delta P_{mf} A = A H_{mf} (\rho_s - \rho_f)(1 - \varepsilon_{mf}) g \tag{1.33}$$

or, eliminating the cross-sectional area

$$\Delta P_{mf} = (\rho_s - \rho_f)(1 - \varepsilon_{mf}) g H_{mf} \tag{1.34}$$

Alternatively equation 1.34 may be thought of as equating the hydrostatic pressure at the base of a column of fluid to the product of bed height, density and the acceleration due to gravity. However, in the case of fluidized solids the density is equal to the difference in density between the particle and the fluidizing medium, the term $(1 - \varepsilon)$ being included because it is only the particles which contribute significantly to the pressure drop. Equation 1.34 allows bed voidage to be determined from experimental measurements of bed pressure drop and bed height. In practice, bed voidage is a function of particle size, particle shape and particle size distribution. Richardson (1971) suggests an approximate value of $\varepsilon_{mf} = 0.4$ for spherical particles. This is perhaps a little low, with values being closer to 0.5 for many particles (Leva, 1959; Kunii and Levenspiel, 1991).

Carman-Kozeny equation

Minimum fluidizing velocity can be predicted from a knowledge of the relationship between the velocity of a fluid passing through a bed of particles and the consequent pressure drop across the bed. However, modelling this relationship is inherently difficult because of the irregular nature of the void spaces in a bed of irregular non-uniformly sized particles; an exact solution is not possible because of the tortuous flow paths followed by the fluid (Figure 1.14). The Carman-Kozeny model is based upon the idea that a packed bed can be modelled by a series of capillaries (Figure 1.15), to which the Hagan-Poiseuille relationship for laminar flow in a tube is applied. By using an equivalent diameter d' and length L' to represent the void spaces, the interstitial velocity u' (i.e. the velocity between the particles in a packed bed) is given by

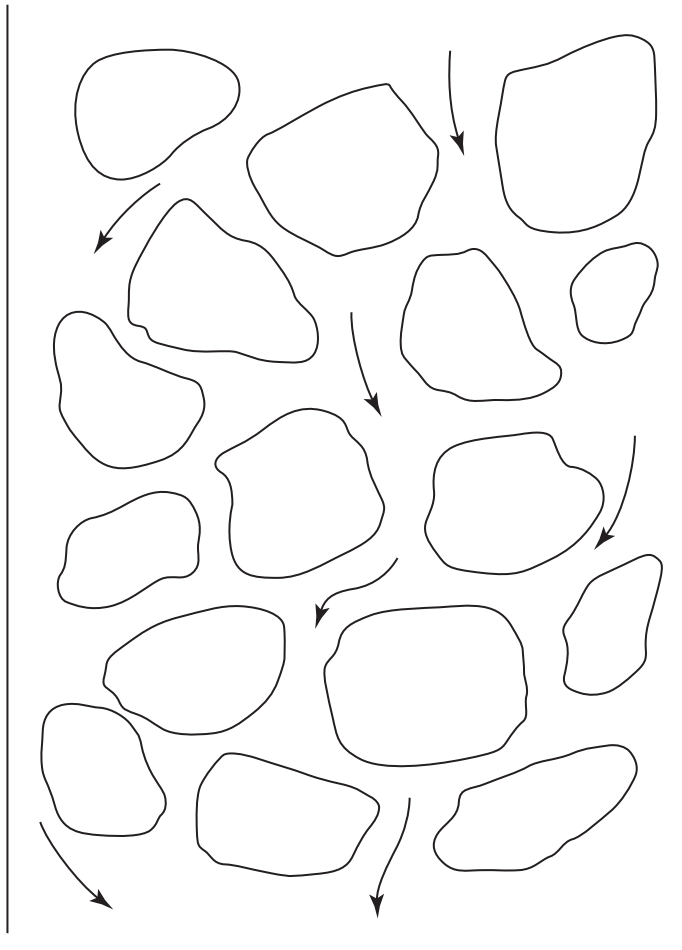

Figure 1.14 Flow path through a packed bed of irregular non-uniformly sized particles.

$$u' = \frac{\Delta P d'^2}{32 L' \mu} \tag{1.35}$$

If now the cross-sectional area which determines the interstitial velocity for a given volumetric flow rate is proportional to the interparticle voidage, it follows that

$$u' = \frac{u}{\varepsilon} \tag{1.36}$$

Kozeny further suggested that the equivalent pore space diameter d' is given by

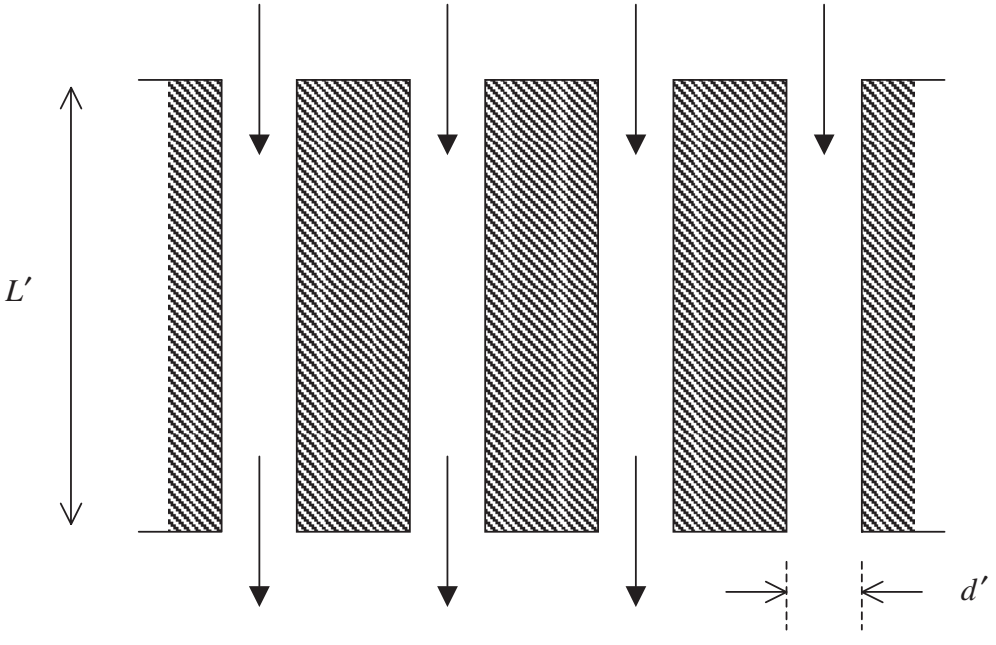

Figure 1.15 Carman-Kozeny model of a packed bed.

$$d' = \frac{\varepsilon}{S_B} \tag{1.37}$$

where S_B is the particle surface area per unit bed volume which comes into contact with the fluid passing through the bed. In turn, this quantity is related to the specific surface by the fraction of the bed occupied by particles $(1 - \varepsilon)$. Thus

$$S_B = S(1-\varepsilon) \tag{1.38}$$

Substituting each of these assumptions into equation 1.35, and further assuming that the equivalent pore space length is proportional to the bed depth H, results in the Carman-Kozeny equation

$$u = \frac{\varepsilon^3 \Delta P}{KS^2(1-\varepsilon)^2 \mu H} \tag{1.39}$$

which relates superficial fluid velocity and pressure drop for a bed of incompressible particles, i.e. for cases where the bed voidage is constant.

The Carman-Kozeny expression for minimum fluidizing velocity is obtained by substituting for the pressure drop at minimum fluidization from equation 1.34 and therefore

$$u_{mf} = \frac{\varepsilon_{mf}^3(\rho_s - \rho_f)g}{KS^2(1-\varepsilon_{mf})\mu} \tag{1.40}$$

The dimensionless constant K is known as Kozeny's constant and has a value of approximately 5.0 although strictly it is a function of both intraparticle porosity and particle shape. Assuming now that the bed particles are spherical for which the specific surface is equal to $\frac{6}{d}$, and that $K = 5$, the minimum fluidizing velocity is given by

$$u_{mf} = \frac{\varepsilon_{mf}^3(\rho_s - \rho_f)gd^2}{180(1-\varepsilon_{mf})\mu} \tag{1.41}$$

This relationship is based on an assumption of laminar flow between particles in a packed bed. Consequently the particle Reynolds number is limited to $Re_{mf} < 20$ (Kunii and Levenspiel, 1991) where

$$Re_{mf} = \frac{\rho_f u_{mf} d}{\mu} \tag{1.42}$$

This corresponds to relatively fine particles, certainly below 500 μm in diameter and perhaps smaller, and thus can be used only for fine food powders, perhaps those encountered in drying and mixing operations, and not for the larger particulates such as vegetable pieces in fluidized bed freezers or large agglomerates in granulation systems. Note that equation 1.41 suggests that u_{mf} is proportional to the difference in density between particle and fluid, proportional to the square of particle diameter and inversely proportional to fluid viscosity.

Ergun equation

The Carman-Kozeny equation works well for fine particles. However, for large particles, greater than about 600 or 700 μm, the Carman-Kozeny relationship is inadequate and predicts far too low a pressure drop. For larger particles, for example peas in a fluidized bed freezer, the minimum fluidizing velocity is high and the kinetic energy losses are significant. In these circumstances the Carman-Kozeny equation vastly overestimates u_{mf} and the Ergun equation is more accurate. This is a semi-empirical equation for the pressure drop per unit bed depth, containing two terms. Ergun's equation may be expressed as

$$\frac{\Delta P}{H} = \frac{150(1-\varepsilon)^2\mu u}{\varepsilon^3\phi^2 d^2} + \frac{1.75(1-\varepsilon)\rho_f u^2}{\varepsilon^3\phi d} \tag{1.43}$$

The first term represents the pressure loss due to viscous drag (this is essentially the Carman-Kozeny equation) whilst the second term represents kinetic energy losses, which are significant at higher velocities (kinetic energy being proportional to velocity squared). Equation 1.43 is valid in the range $1 < Re < 2000$ where the Reynolds number is defined by

$$Re = \frac{u\rho}{S(1-\varepsilon)\mu} \tag{1.44}$$

Writing Ergun's equation for minimum fluidizing conditions, and assuming the particles to be spherical ($\phi = 1$), gives

$$\frac{\Delta P}{H_{mf}} = \frac{150(1-\varepsilon_{mf})^2 \mu u_{mf}}{\varepsilon_{mf}^3 d^2} + \frac{1.75(1-\varepsilon_{mf})\rho_f u_{mf}^2}{\varepsilon_{mf}^3 d} \tag{1.45}$$

and substituting for pressure drop from equation 1.34 gives

$$(\rho_s - \rho_f)g = \frac{150(1-\varepsilon_{mf})\mu u_{mf}}{\varepsilon_{mf}^3 d^2} + \frac{1.75\rho_f u_{mf}^2}{\varepsilon_{mf}^3 d} \tag{1.46}$$

This expression is rather unwieldy but can be simplified considerably. Multiplying through by $\frac{\rho_f d^3}{\mu^2}$ results in

$$\frac{\rho_f(\rho_s - \rho_f)d^3 g}{\mu^2} = \frac{150(1-\varepsilon_{mf})u_{mf} d\rho_f}{\varepsilon_{mf}^3 \mu} + \frac{1.75\rho_f^2 d^2 u_{mf}^2}{\varepsilon_{mf}^3 \mu^2} \tag{1.47}$$

which can be put into the form

$$Ga = \frac{150(1-\varepsilon_{mf})}{\varepsilon_{mf}^3} Re_{mf} + \frac{1.75 Re_{mf}^2}{\varepsilon_{mf}^3} \tag{1.48}$$

This is a quadratic equation in Re_{mf} where the Galileo number Ga is defined by

$$Ga = \frac{\rho_f(\rho_s - \rho_f)d^3 g}{\mu^2} \tag{1.49}$$

and the particle Reynolds number at minimum fluidization by equation 1.42. The Galileo number is also known as the Archimedes number which is usually given the symbol Ar.

Knowledge of the size and density of the particles to be fluidized, of the density and viscosity of the fluidizing gas (at the relevant

temperature) as well as a knowledge of the interparticle voidage at minimum fluidizing conditions (which can be obtained from equation 1.34) allows the Ergun equation to be solved for Re_{mf}. This in turn will permit u_{mf} to be found with the already known values of d, μ and ρ_f. For very large particles the first (viscous drag) term is dominated by the kinetic energy term and it can safely be ignored. Equation 1.48 then reduces to

$$Re_{mf}^2 = \frac{\varepsilon_{mf}^3 Ga}{1.75} \tag{1.50}$$

a slightly more convenient relationship. Kunii and Levenspiel (1991) suggest that such a procedure is valid for $Re_{mf} > 1000$. Smith (2003) and Jackson and Lamb (1981) give worked examples illustrating how both the Ergun and Carman-Kozeny equations can be used to determine the minimum fluidizing velocity of food particulates. Smith demonstrates that for particles with diameters of several millimetres (such as peas or small vegetable pieces), the Carman-Kozeny equation vastly overestimates minimum fluidizing velocity. Further, for such particles, the error in leaving out the viscous drag term in the Ergun equation is small and of the order of 2%.

Minimum fluidizing velocity as a function of terminal falling velocity

Richardson (1971) summarises a method of predicting minimum fluidizing velocity as a function of the terminal falling velocity of a particle. This requires the terminal falling velocity u_t to be expressed in terms of the Galileo number. Thus, treating the Stokes, transition and Newton regions in turn:

(1) For the Stokes region, if equation 1.26 is multiplied by $\frac{\rho_f d}{\mu}$ the result is

$$\frac{\rho_f u_t d}{\mu} = \frac{g(\rho_s - \rho_f) d^3 \rho_f}{18\mu^2} \tag{1.51}$$

which in terms of the Galileo number (equation 1.49) is

$$Re_t = \frac{Ga}{18} \tag{1.52}$$

or

$$Ga = 18 Re_t \tag{1.53}$$

Stokes' law is valid for Reynolds numbers below 0.20 which becomes, for equation 1.53, $Ga < 3.6$.

(2) For the transition region, substituting for the definitions of drag coefficient (equation 1.28) and drag force (equation 1.24) in the Schiller and Naumann equation for drag coefficient gives

$$\frac{\pi}{6} g(\rho_s - \rho_f) d^3 = \frac{\pi d^2}{4} \frac{\rho_f u^2}{2} \frac{24}{Re_t} (1 + 0.15 Re_t^{0.687}) \tag{1.54}$$

When multiplied by $\frac{6\rho_f}{\mu^2}$ this results in

$$\frac{\rho_f g(\rho_s - \rho_f) d^3}{\mu^2} = \frac{18 \rho_f^2 d^2 u^2}{\mu^2} \frac{1}{Re_t} (1 + 0.15 Re_t^{0.687}) \tag{1.55}$$

which in turn becomes

$$Ga = 18 Re_t (1 + 0.15 Re_t^{0.687}) \tag{1.56}$$

and which is valid in the range $3.6 < Ga < 10^5$.

(3) Finally, for the Newton region, at Reynolds numbers greater than 2×10^5, squaring equation 1.32 and multiplying by $\frac{\rho_f^2 d^2}{\mu^2}$ yields

$$\frac{u_t^2 \rho_f^2 d^2}{\mu^2} = (1.74)^2 \frac{\rho_f^2 d^2}{\mu^2} \frac{dg(\rho_s - \rho_f)}{\rho_f} \tag{1.57}$$

In terms of the Reynolds number this becomes

$$Re_t^2 = (1.74)^2 \frac{\rho_f d^3 g(\rho_s - \rho_f)}{\mu^2} \tag{1.58}$$

and hence

$$Ga = 0.33 Re_t^2 \tag{1.59}$$

for Galileo numbers greater than about 10^5. If now the voidage at minimum fluidizing conditions ε_{mf} is known, then for a given value of the Galileo number Ga the ratio of terminal falling velocity to minimum fluidizing velocity $\left(\frac{u_t}{u_{mf}}\right) = \left(\frac{Re_t}{Re_{mf}}\right)$ can be calculated from the Ergun equation and one of equations 1.53, 1.56 or 1.59 respectively. Richardson presents a plot of $\left(\frac{u_t}{u_{mf}}\right) = \left(\frac{Re_t}{Re_{mf}}\right)$ against Ga for commonly

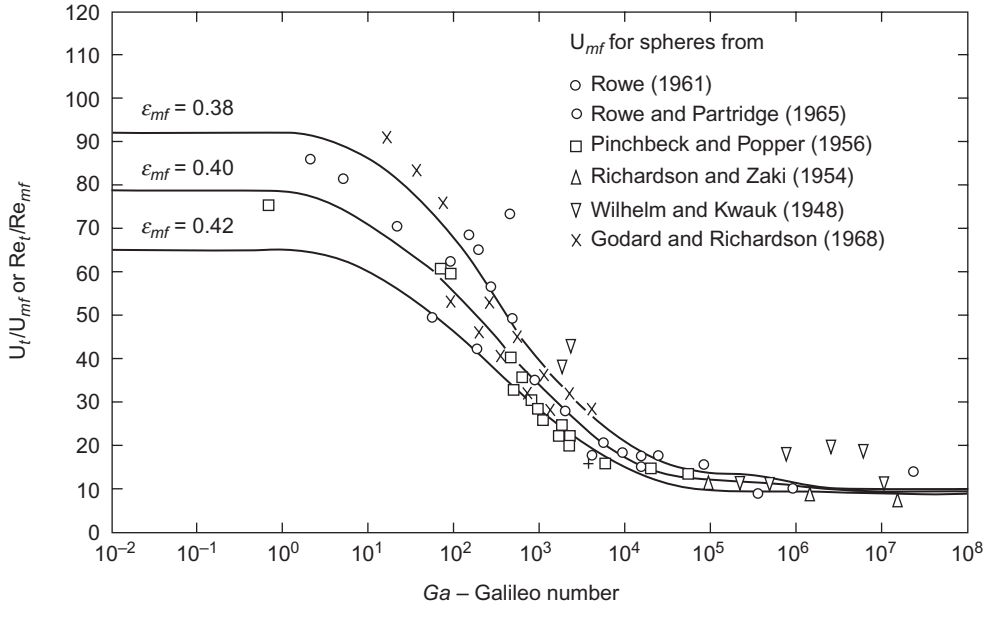

Figure 1.16 Ratio of terminal falling velocity to minimum fluidizing velocity as a function of Galileo number. Reprinted from Davidson, J.F. and Harrison, D., Fluidization, Academic Press, 1971, with permission from Elsevier.

encountered values of voidage (i.e. 0.38, 0.40 and 0.42 respectively) (Figure 1.16). Thus a knowledge of fluid density and viscosity, particle density and diameter allows the calculation of Ga and thus u_{mf}. The values of $\left(\frac{u_t}{u_{mf}}\right)$ are constant for $Ga < 3.6$ and for $Ga > 10^5$; the procedure is rather less convenient in the transition region.

Semi-empirical correlations

Probably the most useful and accurate of the many semi-empirical equations available is that due to Leva

$$u_{mf} = 0.0079 \frac{d^{1.82}(\rho_s - \rho_f)^{0.94}}{\mu^{0.88}} \qquad 1.60$$

This equation allows the prediction of minimum fluidizing velocity from a knowledge of the mean particle diameter, the particle density, the density of fluidizing medium and the viscosity of fluidizing medium (SI units). Couderc (1985) quotes data which show that the inaccuracy of Leva's equation increases significantly outside the range $2 < Re < 30$.

A number of empirical variations on the Ergun equation have been proposed. It can be seen that equation 1.48 is of the form

$$\alpha Re_{mf}^2 + \beta Re_{mf} - Ga = 0 \tag{1.61}$$

This can be rearranged to give

$$Re_{mf} = \left[\left(\frac{\beta}{2\alpha}\right)^2 + \left(\frac{Ga}{\alpha}\right)\right]^{0.5} - \left(\frac{\beta}{2\alpha}\right) \tag{1.62}$$

Recognising that α and β change very little over a very wide range of conditions, a number of workers have fitted experimental data for minimum fluidizing velocity to the Ergun form (Kunii and Levenspiel, 1991). The resulting correlations require neither a knowledge of ε_{mf} nor of ϕ in order for them to be used to predict u_{mf}. Two examples widely used are those due to Wen and Yu (1966) and to Saxena and Vogel (1977), equations 1.63 and 1.64 respectively

$$Re_{mf} = [(33.7)^2 + (0.0408\, Ga)]^{0.5} - 33.7 \tag{1.63}$$

$$Re_{mf} = [(25.3)^2 + (0.0571 Ga)]^{0.5} - 25.3 \tag{1.64}$$

Experimental measurement

The standardised procedure for measuring minimum fluidizing velocity is to fluidize a bed of particles vigorously for some minutes and then reduce gas velocity in small increments to overcome the hysteresis arising from frictional forces in the bed, recording the bed pressure drop each time. This may be done with a simple water manometer with one leg open to atmosphere and one leg connected to a narrow tube placed in the bed and just below the bed surface. The data are then interpreted as in Figure 1.3; u_{mf} corresponds to the intersection of the straight lines representing the fixed and fluidized beds.

Fluidized bed behaviour at high gas velocities

Slugging

As the superficial gas velocity increases, the nature of the bubbles changes. Especially in beds of small diameter or in deep beds, i.e. those with a bed depth to diameter ratio greater than unity, and with fine particles, the bubbles grow to the size of the bed container and push plugs of material up the bed as they rise. The particles then stream past

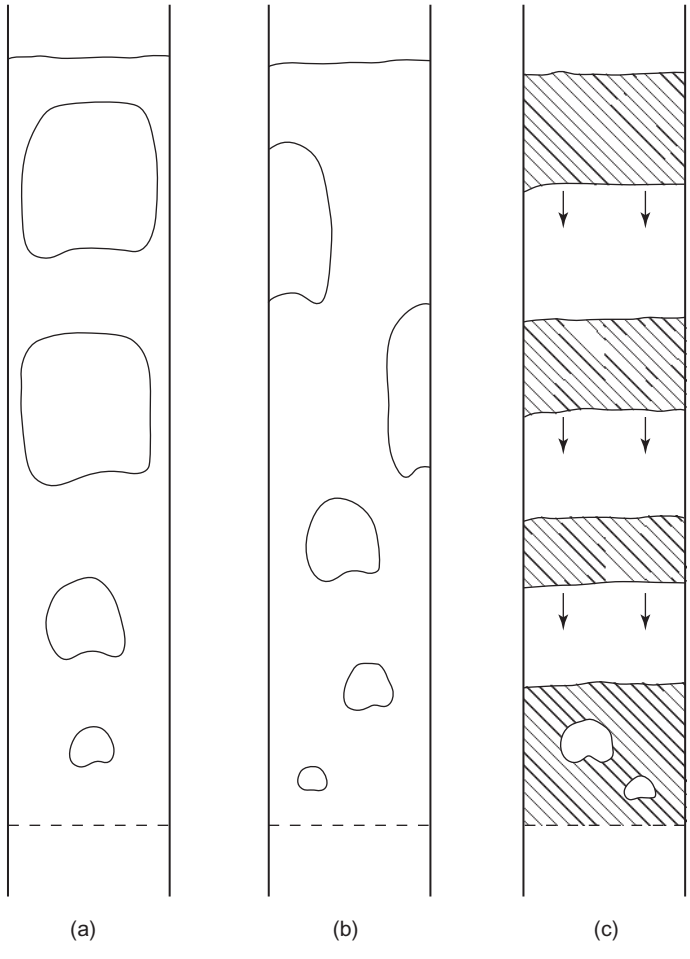

Figure 1.17 Types of slugging behaviour.

the slugs of gas at the bed walls on their downward path as shown in Figure 1.17a. This is known as axial slugging and generally is to be avoided in food processing applications, although it does find application when a fluidized bed is used as a chemical reactor. A single slug tends to rise as would a large bubble in a liquid. Thus the rise velocity is given by a relationship of the form of equation 1.6 but with $k = 0.35$ and is a function of the bed diameter rather than the bubble diameter.

In a second type of slugging behaviour the slugs of gas cling to the wall of the bed as in Figure 1.17b; this tends to occur either with angular particles or when the vessel wall is rough. In the third type of slugging, Figure 1.17c, which occurs with group D particles, there are no distinct bubbles but instead the bed is divided into alternate regions

of dense phase and disperse phase with approximately horizontal interfaces. Particles rain down from one slice of dense phase through a region of disperse phase to the next slice of dense phase below.

Baeyens and Geldart (1974), in an experimental study using a wide range of particle sizes and bed diameters, suggested that generally slugging does not occur below a bed height of H_s given by

$$H_S = 0.6D_{bed}^{0.175} \tag{1.65}$$

where D_{bed} is the bed diameter.

Turbulent fluidization and fast fluidization

As the superficial gas velocity is increased still further the two-phase bed structure, of a bubble or slug phase plus a dense phase, begins to break down and the bed is characterised by significant pressure fluctuations. The bed is now referred to as a turbulent bed where discrete bubbles or slugs are no longer present. There is far more particle ejection into the freeboard and a far less distinct interface between the dense-phase bed and the freeboard. The upper limit of turbulent fluidization is the point where particles are transported out of the column. Elutriated or transported solids must now be recycled to the bed via a cyclone if any solids are to be retained in the fluidized column. If the return feed rate to the bed is low then the solid concentration which results in the bed gives rise to a dilute phase of low concentration which is similar to that found in pneumatic conveying. However, if the solids feed rate is high then a higher concentration of solids can be maintained in the bed and this is known as fast fluidization; gas velocities are very high, at least an order of magnitude greater than the terminal falling velocity. There is an extensive literature on so-called high velocity fluidization, which includes both turbulent and fast fluidization. However, as with slugging, there are few if any applications involving food materials and these regimes are relevant only to heterogeneous chemical reactors.

Elutriation and entrainment

In any fluidized bed operating with a gas velocity above u_{mf} some particles will be transported into the gas stream above the bed surface; this is called entrainment. Some of these particles will be transported sufficiently so as to leave the fluidized bed column entirely and this mass of solids is then referred to as carry-over. However, the phenomenon is a little more complex. Fractionation or preferential separation of the bed particles occurs and this changes with height above the bed

surface; it is this phenomenon which is called elutriation. In a bed with a distribution of particle sizes, and most fluidized beds of real interest come into this category, only the smallest particles are removed and form a disperse phase which occupies the freeboard. The freeboard is the term given to the space between the surface of the dense phase and the point at which gas exits the column. It is important to differentiate, however, between the disperse phase and so-called dilute-phase fluidization where all the particulate solids are carried in the gas stream and which corresponds to one of the regimes of pneumatic conveying.

Elutriation is important in most industrial fluidized beds and is generally thought of as a disadvantage. In addition to the small particles which may be present in the initial particle size distribution, fines may be created in the course of operation by the attrition of bed particles. Elutriated particles usually need to be collected and recovered either because they represent the loss of product particles of a given size, because they must be separated from the exhaust gas for environmental reasons, or because of safety concerns; there is a considerable risk of a dust explosion with very fine particles and perhaps especially so with many food particulates. Therefore the fluidized bed plant will require ancillary gas cleaning equipment such as a cyclone, filter or electrostatic precipitator to separate the fines from the gas. The loss of a particular size fraction from the bed may change fluidized bed behaviour and it then becomes important to return the fines to the bed continuously.

Elutriation can occur only if the terminal falling velocity of a particle is exceeded. Particles are brought to the surface of the bed by the rising gas bubbles which carry particles up the bed in the bubble wake and the eruption of the bubbles at the dense phase surface then throws particles up into the freeboard where the local velocity is at least approximately equal to the superficial velocity and possibly higher. In addition, gas bubbles rise through the bed at a velocity higher than that of the surrounding dense phase and also the pressure in the bubble is very slightly higher than the surrounding interstitial gas. These factors explain why the particles in the bubble wake material are thrown into the freeboard as packets of particles. The fines are then carried up in the gas stream and the larger particles fall back.

There is, however, considerable variation across a bed diameter in the velocity of the gas leaving the surface of the bed simply because any given bed cross-section contains both bubble phase and lean phase (Figure 1.18). As the gas travels up the column these variations in velocity become less pronounced and therefore the larger particles fall back as the local velocity falls below their terminal falling velocity. The height above the bed surface at which the larger particles disengage is

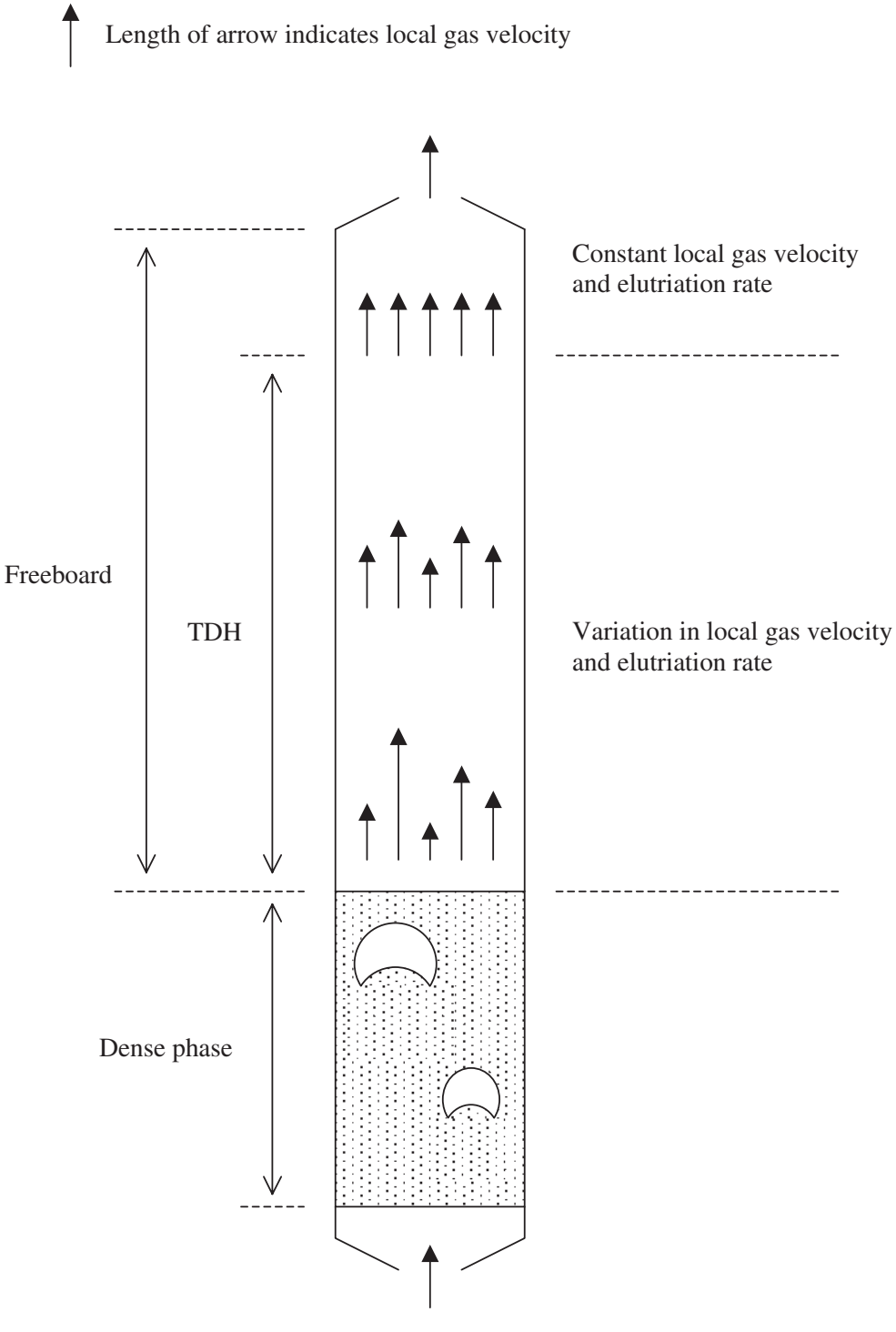

Figure 1.18 Elutriation and transport disengaging height (TDH).

called the transport disengaging height (TDH). Alternatively the TDH may be defined as the height at which the elutriation rate, and therefore the particle size distribution of the elutriated particles, is approximately constant. The TDH increases with both superficial gas velocity and with bed diameter; the latter effect is due to wall effects at small bed diameters and to relatively poor gas distribution at larger bed diameters. The concentration of solids decreases with height above the bed surface and therefore increasing the height of the freeboard reduces the loss of particles from the bed. In other words, when the gas exit is above the TDH the rate of solids loss is constant and therefore it is common to design the freeboard height to be equal to TDH.

Other types of fluidization

Spouted beds

A spouted bed requires a cylindrical container with an inverted conical base and a vertical pipe entering at the apex of the cone. If coarse solids are placed in the container and gas is introduced through the pipe, the solids will begin to 'spout' as in Figure 1.19. Particles are carried at high velocity upwards in the central jet in a dilute phase and at the bed surface the particles form a kind of fountain and rain down onto the clearly defined surface. They then travel down the bed in the annulus at much lower velocities than those in the central spout. On reaching the gas inlet point, the particles are re-entrained and thus complete a well-defined and regular cycle. Spouted beds can exist only with large particles, usually greater than 1–2 mm in diameter. A uniform particle size distribution is more likely to result in spouting bed behaviour, although particles with a larger mean diameter will spout more readily with a wider size distribution than will smaller particles. If the cone is too steep then the bed becomes unstable; the limiting cone angle is about 40°. Particle motion is much more regular than in a fluidized bed although there is a distribution of cycle times with particles re-entering the spout at various points up the bed.

As in the case of fluidization, there is a gas velocity below which spouting does not occur. The earliest and best known relationship to predict the minimum spouting velocity u_{ms} is that due to Mathur and Gishler (1955)

$$u_{ms} = \left(\frac{d}{D_{bed}}\right)\left(\frac{D_i}{D_{bed}}\right)^{0.33}\left(\frac{2gH(\rho_s - \rho_f)}{\rho_f}\right)^{0.5} \qquad 1.66$$

which indicates that the minimum spouting velocity increases with bed depth H but decreases with bed diameter D_{bed} and that it increases

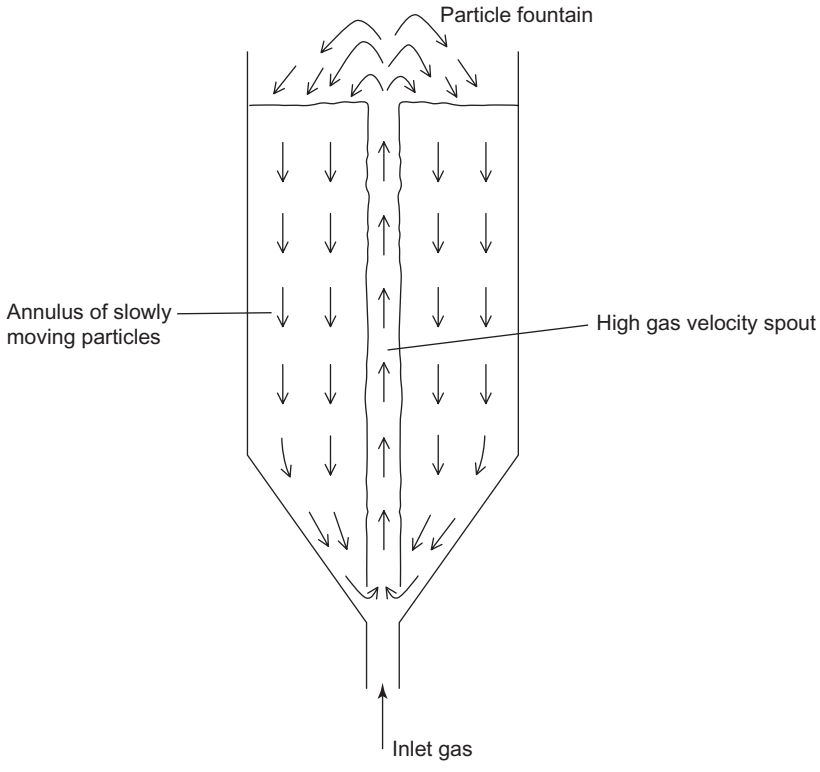

Figure 1.19 Spouted bed.

slightly with the diameter of the gas inlet D_i. The pressure drop down the bed is not uniform; it is small at the base and reaches a maximum at the surface where it approaches the pressure drop needed to support the solids. If the gas velocity is sufficient to fluidize the particles then the spouted bed becomes unstable; thus there is a maximum spoutable depth H_{sm} beyond which spouting behaviour breaks down and the bed becomes fluidized. Mathur (1971) suggests that u_{ms} is approximately equal to the minimum fluidizing velocity when the bed depth is close to the maximum spoutable depth. However, because in practical situations the bed depth would be considerably less than this maximum, gas velocities required for spouting are somewhat less than those required for fluidization. Data are available (Mathur, 1971) for a variety of solids, including wheat, mustard seed, rape seed, millet and peas, for all of which equation 1.66 has been shown to be valid. The simplest way to determine H_{sm} is to calculate, or measure, the minimum fluidizing velocity of the bed particles and then substitute this figure for u_{ms} in equation 1.66, solving for H. Predicted values of maximum spoutable depth obtained with this approach are in agreement with experimental data (Mathur, 1971). The applications of spouted beds

include drying, particularly the drying of wheat, granulation and the coating of seeds and large particles.

Centrifugal fluidization

The so-called centrifugal fluidized bed has found application in the drying of foods and is claimed to give stable and smooth fluidization of large irregular particles at velocities well above those required for pneumatic transport. Its particular advantage is that high gas velocities allow significant heat input to the bed at lower temperatures than would otherwise be needed and hence the high rates of heat transfer which become possible in the constant drying rate zone of a drying process allow the centrifugal bed to be used for the reduction of initial moisture in sticky, high-moisture, heat-sensitive foods (Carlson *et al*., 1976).

Hanni *et al*. (1976) described a continuous fluidized bed drier using the centrifugal principle. It consisted of a perforated horizontal cylinder rotating inside a plenum with hot air blown across the outside of the cylinder and perpendicular to the axis of rotation (Figure 1.20). Vanes placed in the air inlet allowed the incident angle of the air flow to be varied from 0° to 45° to the perpendicular. Particles were fluidized inside the Teflon-coated stainless steel cylinder which could be tilted by up to 6° in order to control particle residence time. The cylinder, of

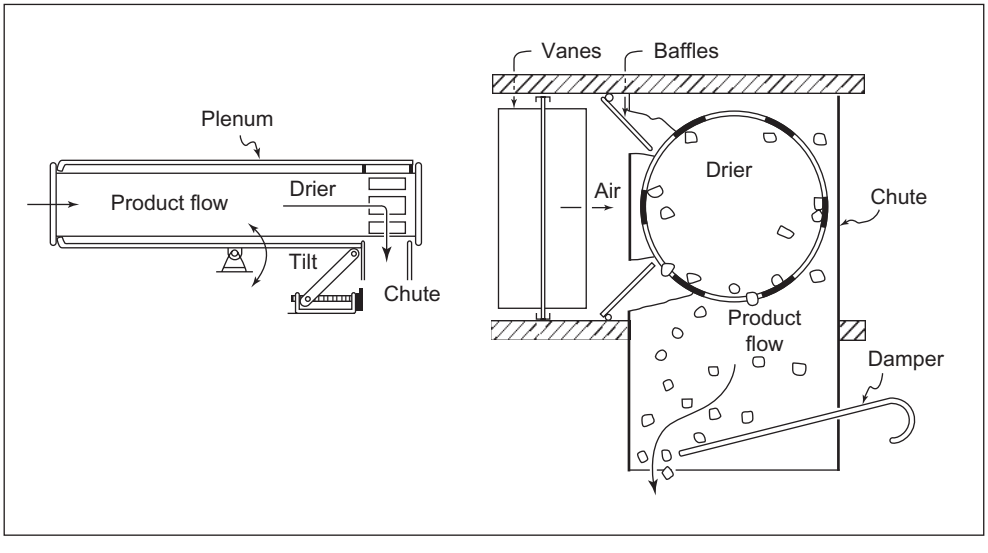

Figure 1.20 Centrifugal fluidized bed. From Hanni *et al*. (1976), by permission of the Institute of Food Technologists, USA.

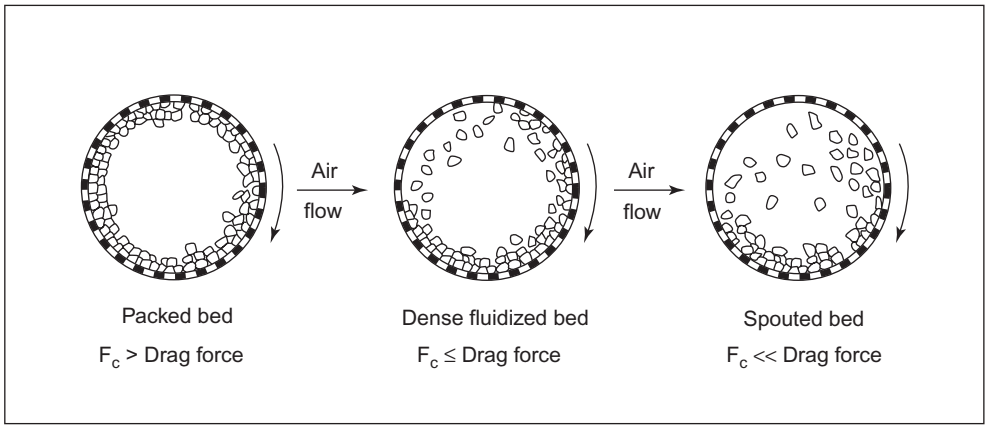

Figure 1.21 Fluidization regimes in a centrifugal fluidized bed. From Hanni *et al*. (1976), by permission of the Institute of Food Technologists, USA.

diameter 0.25 m and length 2.5 m, was perforated with 2.4 mm diameter holes giving an open area of 45% and rotated at speeds up to 350 rpm (5.8 Hz). The plenum was divided into two equal lengths, allowing different drying conditions in the feed zone and the discharge zone of the bed respectively. Air passed through the perforations of the drying cylinder and left the plenum to be reheated and recirculated. Mechanical details of sealing the air flow and the control of air velocity are also given.

Hanni *et al*. (1976) used the centrifugal fluidized bed for drying diced vegetables of approximately 10 mm in size with the wet feed being blown into the fluidized bed with air. The perforated surface of the cylinder acted as the distributor plate and the centrifugal action kept the particle bed in place close to the cylinder wall. They suggested that the feed end of the bed was characterised by dense-phase fluidization with partially dried material being displaced by fresh feed and passing on to the second half or discharge end of the cylinder. Here the particle bed approached spouted bed conditions before the particles were discharged radially from the bed by pneumatic transport (Figure 1.21).

Particulate fluidization

Particulate fluidization, where the fluidizing medium is usually a liquid, is characterised by a smooth expansion of the bed. Liquid-solid fluidized beds are used in continuous crystallisers, as bioreactors in which immobilised enzyme beads are fluidized by the reactant solution and in physical operations such as the washing and preparation of vegetables. The empirical Richardson–Zaki equation (Richardson

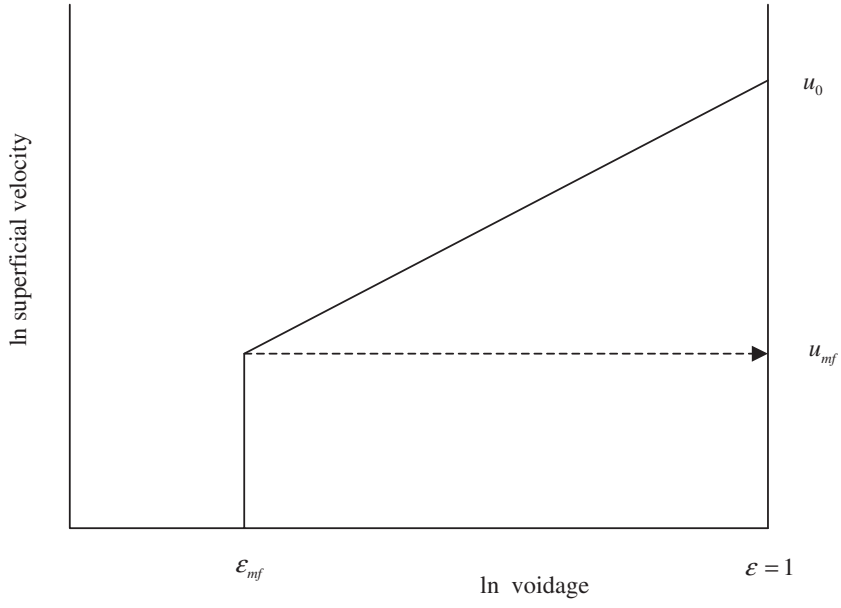

Figure 1.22 Richardson–Zaki plot: measurement of minimum fluidizing velocity for particulate fluidization.

and Zaki, 1954) describes the relationship between the superficial fluid velocity and bed voidage

$$\frac{u}{u_0} = \varepsilon^n \tag{1.67}$$

where u_0 is the superficial velocity at a voidage of unity and n is an index which depends on the particle Reynolds number. Figure 1.22 shows the form of a logarithmic plot of velocity against voidage. The vertical line represents the packed bed where the bed voidage does not change with velocity. The inclined section of the plot represents the fluidized bed, described by equation 1.67, and has a gradient equal to n. The minimum fluidizing velocity is found at the intersection of the two lines. The value of n is usually in the range 2.4–5.0, with smaller values at higher Reynolds numbers. There is a degree of similarity between the fluidization of a particle and the settling of a particle in a fluid. For sedimentation $u_0 = u_t$, i.e. the velocity at a voidage of unity is equal to the terminal falling velocity. However, in particulate fluidization a wall effect exists and

$$\ln u_0 = \ln u_t - \frac{d}{D_{bed}} \tag{1.68}$$

Table 1.2 Richardson–Zaki index as a function of Reynolds number.

$Re < 0.2$	$n = 4.65 + 20\dfrac{d}{D_{bed}}$
$0.2 < Re < 1$	$n = \left(4.4 + 18\dfrac{d}{D_{bed}}\right) Re^{-0.03}$
$1 < Re < 200$	$n = \left(4.4 + 18\dfrac{d}{D_{bed}}\right) Re^{-0.1}$
$200 < Re < 500$	$n = 4.4\,Re^{-0.1}$
$Re > 500$	$n = 2.4$

where D_{bed} is the bed diameter. Thus as the bed diameter increases relative to the particle diameter, fluidization behaviour approaches that of a sedimenting particle. Richardson and Zaki (1954) proposed a series of empirical equations for the relationship between n and Reynolds number; these are listed in Table 1.2. For non-spherical particles, for example vegetable pieces, the value of n will be higher than for spheres; here Richardson and Zaki suggested

$$n = 2.7K''^{0.16} \quad (\text{for } Re > 500) \tag{1.69}$$

where the shape factor K'' is defined by equation 1.15.

The Richardson–Zaki equation has been found to agree with experimental data over a wide range of conditions. Equally, it is possible to use a pressure drop–velocity relationship such as Ergun to determine minimum fluidization velocity, just as for gas-solid fluidization. An alternative expression, which has the merit of simplicity, is that of Riba *et al*. (1978)

$$Re_{mf} = 1.54 \times 10^{-2} Ga^{0.66} \left(\frac{\rho_s - \rho_f}{\rho_f}\right)^{0.7} \tag{1.70}$$

which is valid in the Reynolds number range $10 < Re < 1000$.

Nomenclature

A bed cross-sectional area
c_D drag coefficient
d mean particle diameter
d_B bubble diameter
d_e equivalent spherical diameter
d_s diameter of a sphere with the same surface area as particle
d_p diameter of a circle having an area equal to the projected area of particle in its most stable position

d' equivalent diameter of void spaces
D_{bed} bed diameter
D_i diameter of spouted bed gas inlet
F drag force
Fr Froude number
g acceleration due to gravity
Ga Galileo number
H bed height
H_{mf} bed height at minimum fluidization
H_S minimum bed height for slugging
H_{sm} maximum spoutable bed depth
k constant in equation 1.6
K Kozeny's constant
K' volume shape factor
K'' shape factor defined by equation 1.15
L' equivalent length of void spaces
m particle mass
m' mass of displaced fluid
n index in Richardson–Zaki equation
N number of particles of size x
p parameter representing characteristic of a particle size distribution
q parameter representing characteristic of a particle size distribution
Q total volumetric gas flow rate
Q_B volumetric bubble flow rate
Q_{mf} volumetric gas flow rate at minimum fluidization
Re Reynolds number
Re_t Reynolds number at terminal falling velocity
S specific surface
S_B particle surface area per unit bed volume in contact with fluid
t time; average particle circulation time
u superficial velocity; velocity through aperture of distributor plate; relative velocity between sphere and fluid
u_B bubble rise velocity
u_{mb} minimum bubbling velocity
u_{mf} minimum fluidizing velocity
u_{ms} minimum spouting velocity
u_{SB} rise velocity of a single bubble
u_t terminal falling velocity
u' interstitial velocity
u_0 superficial velocity at a voidage of unity
V particle volume
x particle size

x_l lower limit of size distribution
x_u upper limit of size distribution
$x_{3,2}$ surface–volume mean diameter

Greek symbols

α coefficient in generalised Ergun equation
β coefficient in generalised Ergun equation
ΔP bed pressure drop
ΔP_d pressure drop across distributor plate
ε interparticle voidage
μ viscosity
ρ_B bulk density
ρ_f gas density
ρ_s particle density
ϕ sphericity
ω mass fraction of particles of a given size

Subscripts

f fluid
mf minimum fluidizing conditions
s solid

References

Abrahamson, A.R. and Geldart, D., Behaviour of gas-fluidized beds of fine powders part I. Homogeneous expansion, *Powder Tech*., **26** (1980) 35–46.

Allen, T., Particle size measurement, Chapman and Hall, London, 1981.

Arjona, J.L., Rios, G.M. and Gibert, H., Two new techniques for quick roasting of coffee, *Lebensmittel Wissenschaft Technologie*, **13** (1980) 285–290.

Baeyens, J. and Geldart, D., An investigation into slugging fluidized beds, *Chem. Eng. Sci*., **29** (1974) 255–265.

Botterill, J.S.M., Fluid-bed heat transfer, Academic Press, London, 1975.

Carlson, R.A., Roberts, R.L. and Farkas, D.F., Preparation of quick-cooking rice products using a centrifugal fluidized bed, *J. Food Sci*., **41** (1976) 1177–1179.

Couderc, J.-P., Incipient fluidization and particulate systems, in: Davidson, J.F., Clift, R. and Harrison, D., (eds.), Fluidization, 2nd ed., Academic Press, London, 1985.

Davidson, J.F. and Harrison, D., Fluidised particles, Cambridge University Press, Cambridge, 1963.

Davidson, J.F. and Harrison, D., (eds.), Fluidization, Academic Press, London, 1971.

Davidson, J.F., Clift, R. and Harrison, D., (eds.), Fluidization, 2nd ed., Academic Press, London, 1985.

Epstein, N., Applications of liquid-solid fluidization, *Int. J. Chem. Reactor Eng.*, **1** (2003) 1–16.

Geldart, D., Types of gas fluidization, *Powder Tech.*, **7** (1973) 285–292.

Geldart, D., Mixing in fluidized beds, in: Harnby, N., Edwards, M.F. and Nienow, A.W., (eds.), Mixing in the process industries, Butterworth-Heinemann, Oxford, 1992.

Gibilaro, L.G., Fluidization-dynamics: the formulation and applications of a predictive theory for the fluidized state, Butterworth-Heinemann, Oxford, 2001.

Hanni, P.F., Farkas, D.F. and Brown, G.E., Design and operating parameters for a centrifugal fluidized bed drier, *J. Food Sci.*, **41** (1976) 1172–1176.

Hiby, J.W., Untersuchungen über den kritischen Mindestdruckverlust des Anströmbodens bei Fluidalbetten (Fließbetten) [Examination of the critical minimum pressure loss in a fluidised bed], *Chem. Ing. Techn.*, **36** (1964) 228–229.

Jackson, A.T. and Lamb, J., Calculations in food and chemical engineering, Macmillan, Basingstoke, 1981.

Jonke, A.A., Petkus, E.J., Loeding, J.W. and Lawroski, S., Calcination of dissolved nitrate salts, *Nucl. Sci. Eng.*, **2** (1957) 303–319.

Jowitt, R., Heat transfer in some food processing applications of fluidisation, *Chem. Engnr.*, **November** (1977) 779–782.

Kunii, D. and Levenspiel, O., Fluidization engineering, Butterworth-Heinemann, Oxford, 1991.

Leva, M., Fluidization, McGraw-Hill, New York, 1959.

Mathur, K.B., Spouted beds, in: Davidson, J.F. and Harrison, D., (eds.), Fluidization, Academic Press, London, 1971.

Mathur K.B. and Epstein, N., Spouted beds, Academic Press, New York, 1974.

Mathur, K.B. and Gishler, P.E., A technique for contacting gases with coarse solid particles, *A.I.Chem.E.J.*, **1** (1955) 157–164.

Mishra, I.M., El-Temtamy, S.A. and Schugerl, K., Growth of *Saccharomyces cerevisiae* in gaseous fluidized beds, *Eur. J. Appl. Microbiol. Biotechnol.*, **16** (1982) 197–203.

Mugele, R.A. and Evans, H.D., Droplet size distribution in sprays, *Ind. Eng. Chem.*, **43** (1951) 1317–1324.

Mullin, J.W., Crystallization, 3rd ed., Butterworth-Heinemann, Oxford, 1993.

Rankell, A.S., Scott, M.W., Lieberman, H.A., Chow, F.S. and Battista, J.V., Continuous production of tablet granulations in a fluidized bed II. Operation and performance of equipment, *J. Pharm. Sci.*, **53** (1964) 320–324.

Riba, J.P., Routie, R. and Couderc, J.P., Conditions minimales de mise en fluidisation per une liquide [Minimum conditions for initiation of fluidisation with a liquid], *Can. J. Chem. Eng.*, **56** (1978) 26–34.

Richardson, J.F., Incipient fluidization and particulate systems, in: Davidson, J.F. and Harrison, D., (eds.), Fluidization, Academic Press, London, 1971.

Richardson, J.F. and Zaki, W.N., Sedimentation and fluidisation. Part 1, *Trans. Inst. Chem. Engrs.*, **32** (1954) 35–52.

Rios, G.M., Gibert, H. and Baxerres, J.L., Factors influencing the extent of enzyme inactivation during fluidized bed blanching of peas, *Lebensmittel Wissenschaft Technologie*, **11** (1978) 176–180.

Rios, G.M., Gibert, H. and Baxerres, J.L., Potential applications of fluidisation to food preservation, in: Thorne, S., (ed.), Developments in food preservation, volume 3, Elsevier, Amsterdam, 1985, 273–304.

Rowe, P.N., Experimental properties of bubbles, in: Davidson, J.F. and Harrison, D., (eds.), Fluidization, Academic Press, London, 1971.

Rowe, P.N., Estimation of solids circulation rate in a bubbling fluidised bed, *Chem. Eng. Sci*., **28** (1977) 979–980.

Saxena, S.C. and Vogel, G. J., The measurement of incipient fluidisation velocities in a bed of coarse dolomite at temperature and pressure, *Trans. Inst. Chem. Engrs*., **55** (1977) 184–189.

Schiller, L. and Naumann, A.Z., Uber die grundlegenden Berechnungen bei der Schwerkraftaufbereitung [A fundamental drag coefficient correlation], *Z. Ver. Deut. Ing*., **77** (1933) 318–320.

Sherrington, P.J. and Oliver, R., Granulation, Heyden, London, 1981.

Shi, Y.F. and Fan, L.T., Effect of distributor to bed resistance ratio on uniformity of fluidization, *A.I.Ch.E.J*., **30** (1984) 860–865.

Shilton, N.C. and Niranjan, K., Fluidization and its applications to food processing, *Food Structure*, **12** (1993) 199–215.

Siegel, R., Effect of distributor plate-to-bed resistance ratio on onset of fluidized bed channelling, *A.I.Ch.E.J*., **22** (1976) 590–592.

Smith, P.G., Introduction to food process engineering, Kluwer Academic, New York, 2003.

Smith, P.G. and Nienow, A.W., Particle growth mechanisms in fluidised bed granulation – part I. The effect of process variables, *Chem. Eng. Sci*., **38** (1983) 1223–1231.

Stokes, G.G., On the effect of the internal friction of fluids on the motion of pendulums, *Trans. Cambridge Phil. Soc*., **9** (1851) 8–106.

Vinter, H., Aqueous (and organic) film-coating by fluidisation technology, Proceedings of an International Conference on Fluidisation Technology for Pharmaceutical Manufacturers, Powder Advisory Centre, London, 1982, 1–11.

Wen, C.J. and Yu, Y.H., A generalized method for predicting the minimum fluidization velocity, *A.I.Ch.E.J*., **12** (1966) 610–612.

Wilhelm, R.H. and Kwauk, M., Fluidization of solid particles, *Chem. Eng. Prog*., **44** (1948) 201–218.

Yates, J.G., Fundamentals of fluidized-bed chemical processes, Butterworth, London, 1983.

Yerushalmi, J. and Avidan, A., High-velocity fluidization, in: Davidson, J.F., Clift, R. and Harrison, D., (eds.), Fluidization, 2nd ed., Academic Press, London, 1985.

Zenz, F.A., Regimes of fluidized behaviour, in: Davidson, J.F. and Harrison, D., (eds.), Fluidization, Academic Press, London, 1971.